MASTER COPY

OAK RIDGE NATIONAL LABORATORY

operated by

UNION CARBIDE CORPORATION

for the

U.S. ATOMIC ENERGY COMMISSION

ORNL-TM-69

COPY NO. - 4

DATE - December 4, 1961

Neutron Activation Calculations for the Transuranium Laboratory

J. P. Nichols

ABSTRACT

Neutron activation and flux calculations performed as an aid to the Transuranium Laboratory design are reported. The degree of activation as a function of irradiation and decay time was evaluated on the ORACLE for shielding window materials, magnetite concrete, steels, aluminums, Hastelloys, and various other alloys. The neutron flux in concrete cells was evaluated using multigroup reactor codes.

NOTICE

This document contains information of a preliminary nature and was prepared primarily for internal use at the Oak Ridge National Laboratory. It is subject to revision or correction and therefore does not represent a final report. The information is not to be abstracted, reprinted or otherwise given public dissemination without the approval of the ORNL patent branch, Legal and Information Control Department.

1.0 SUMMARY

Neutron activation and flux calculations have been made for structural and shield materials that may be exposed to neutron sources in the Transuranium Laboratory. The calculations were performed on the ORACLE using known cross sections, half-lives and decay schemes. The multigroup neutron flux within cells was calculated on the IBM-7090 using the DSN and GNU codes. Estimates of the activation problems that may occur in the Laboratory are presented along with methods of calculation and data which may be used for the evaluation of specific problems in the future. Significant results and conclusions of the study are as follows:

1. The thermal flux inside a cell is approximately 1/4 the fast flux at the cell wall.
2. Inclusion of 2.5 lbs of boron per cubic yard of magnetite concrete will lower the thermal flux in the cell to 1/10 the fast flux at the cell wall. It is infeasible to add additional boron to the concrete since fast activation begins to control at this level.
3. The coating of tanks which contain solutions of neutron emitting materials with 15-20 mils of Cd and inclusion of 2.5 lbs boron/cu yd in the surrounding concrete walls will lower the activation of adjacent tanks and structural materials approximately an order of magnitude below that to be encountered without the use of thermal poisons.
4. The gamma flux from the concrete walls of pits, which could be exposed to fast and thermal neutron fluxes of $\sim 10^8$ for long periods, would be equivalent to 50-200 mr/hr for decay times of 1-100 days.
5. The gamma flux from the concrete walls in cubicle cells, which will only be exposed to high-level neutron sources for short periods, will be in the order of 1-20 mr/hr for decay times of 1-100 days.
6. The activation activity of oil-filled glass windows is very short lived; although the surface dose rate is many rem/hr at decay times less than 1 day, it is insignificant for decay times greater than 10 days.
7. Zinc bromide windows become considerably activated. Windows exposed to sources such as will be present in the Transuranium

Laboratory would have to be compartmentalized to prevent radioactive solution from circulating to the operating face and causing dose rates of several rem per hour.

8. A CRL Model D manipulator exposed to a source of several hundred mg of Cf^{252}-Cf^{254} for 10 days would survey approximately 2000, 10, and 1 mr/hr after decay times of 1 hr, 1 day, and 100 days, respectively.
9. The conditions of neutron exposure to the dissolver, mixer-settlers, and californium storage tank may be such that the gamma dose rate at the surface after 10-100 days decay time is 30, 200, and 20,000 mr/hr, respectively.
10. Stainless steel equipment racks and tanks adjacent to the californium storage tank would survey 100-200 mr/hr for decay times of 1-100 days if thermal neutron poisons are not used.

2.0 INTRODUCTION

Neutron activation calculations have been made for structural and shield materials that may be exposed to α-n and spontaneous fission neutron sources in the Transuranium Laboratory. This report is intended to present calculational methods, data, and an order-of-magnitude survey of the activation problems that will occur in the Transuranium Laboratory. The methods and data may be applied later to give more accurate results for specific problems in which the materials, geometry, and source strengths are specified.

The activation data for specific materials was generated on the ORACLE using isotopic abundancies, fast and thermal cross sections, half lives, and decay schemes for components of the materials taken from Sullivan's chart[1], ORNL-2125[2], and Radiation Shielding.[4] The fast and thermal flux resulting from fission sources were calculated on the IBM-7090 using DSN, and 18-group transport code, and GNU, a 32 group diffusion code. The materials for which activation calculations were made are 3.3 density lead silicate glasses, 2.7 density non-browning glass, 6.2 density lead glasses, zinc bromide solution, magnetite concrete, stainless steel 304L and 440A, Hastelloy "B" and "C", aluminum 356, 1050, 2024, and 6061, Monel carbon steel, Elgiloy, and Almag 35.

Acknowledgments are due to D. A. Griffin, who coded the activation equations and prepared the input for the ORACLE, and G. E. Whitesides, who prepared the input for DSN and GNU.

3.0 ASSUMPTIONS AND METHODS OF CALCULATION ACTIVATION EQUATIONS

The degree of activation and gamma dose rate at the surface of a slab was calculated for various materials subjected to a constant flux as a function of irradiation time and decay time. The calculations were performed for a flux of 10^{10} neutrons/cm^2-sec, which is near the flux that will be encountered in Transuranium Laboratory cells; the degree of activation and dose rate for other values of flux may be obtained through the use of a direct proportion. The dose rate at the surface of a slab was calculated assuming that the flux in the first 10-20 cm of the material is constant; for the materials that are evaluated consideration of the fast and thermal flux perturbation would not lower the calculated dose rate more than approximately a factor of two. The slab thickness was chosen to correspond approximately with the thickness that will be used in the Transuranium Laboratory.

The mechanism of activation is (isotope i-1) stable + neutron $\longrightarrow$ (isotope i) radioactive. The nomenclature that is used in writing the activation equations is as follows:

ϕ	= fast or thermal neutron flux = 10^{10} neutrons/cm^2-sec
T	= time in which material is exposed to neutron flux, sec
t	= decay time after exposure to flux, sec
λ_i	= decay constant of element i, sec^{-1}
W_i-1	= density of element of isotopes i-1 in material, g/cc
X_i-1	= fraction of isotope i-1 in element
σc_i-1	= fast or thermal activation cross section of isotope i-1, barns
M_i-1	= molecular weight of isotope i-1
$A_i(T,t)$	= gamma activation activity of isotope i, γdis/sec-cc
n	= number of stable isotopes in subject material
A(T,t)	= total γ activation activity of material, γ dis/sec-cc
ρ	= density of the subject material, g/cc
Z	= Thickness of a slab of the subject material, cm
$\mu(E)$	= gamma attenuation coefficient of the subject material for gamma ray of energy E_{ij}, cm^2/gm
E_{ij}	= gamma ray energy resulting from one mode of disintegration of isotope i.

m = number of gamma modes of disintegration of isotope i

y_{ij} = fraction of occurrence of gamma of energy E_{ij} per disintegration of isotope i

d_{ij} = gamma dose rate at the surface of a slab of the subject material resulting from disintegrations of gamma ray energy E_{ij}, mr/hr

$D(T,t)$ = total gamma dose rate at the surface of a slab of the subject material, mr/hr

The activation equations are

$$A(T,t) = \sum_{i=1}^{i=n} \frac{(W_i-1)X_i-1)(.6023)(\sigma c_i-1)(\emptyset)(1-e^{-\lambda_i T})(e^{-\lambda_i t})}{(M_i-1)} \tag{1}$$

$$d_{ij}(T,t) = \frac{A_i(T,t)y_{ij}E_{ij}}{2\mu\rho\ (580)} \quad \text{for } Z > \frac{1}{\mu\rho} \tag{2}$$

$$d_{ij}(T,t) = \frac{A_i(T,t)y_{ij}E_{ij}Z}{(2)(580)} \quad \text{for } Z \leq \frac{1}{\mu\rho} \tag{3}$$

$$D(T,t) = \sum_{i=1}^{i=n} \sum_{j=1}^{j=m} d_{ij} \tag{4}$$

The equations for $A(T,t)$ and $D(T,t)$ were solved on the ORACLE using the properties of materials listed in Table 1, and properties of isotopes listed in Table 2.

Flux Calculations

The 18 and 32 group neutron flux was calculated in cells, concrete walls, and in the vicinity of a 100-liter spherical tank. The cell geometry was considered to consist of a spontaneous fission neutron source of 10^{14} neutrons/sec at the center of an 8-ft-dia air-filled sphere, which in turn was surrounded by a 6-ft-thick magnetite concrete wall. The density of the various elements in the concrete in grams per cc were assumed as follows: H = 0.0217, O = 1.255, Mg = 0.0326, Al + Si + Ca = 0.4246 (Al cross sections used), Fe + Ti + V = 1.878

Table 1. Properties of Structural and Shield Materials

Material	Component Elements	W_i-1 g/cc	Z cm
Lead	O	1.04	
Silicate	Na	0.137	
Glass	Al	0.047	50
# 1	Si	0.[illegible]	
ρ = 3.30	K	0.373	
	Ce	0.044	
	Pb	0.972	
Nonbrowning	Si	0.[illegible]	
Glass	B	0.025	
(PPG 0740)	Na	0.130	
ρ = 2.70	Ba	0.342	1
	K	0.202	
	Ce	0.037	
	O	1.125	
Magnetite	H	0.0217	
Concrete	O	1.275	
ρ = 3.62	Mg	0.033	
	Al	0.063	
	Si	0.091	
	P	0.0004	50
	S	0.0052	
	Ca	0.250	
	Ti	0.192	
	V	0.0113	
	Cr	0.0057	
	Mn	0.0067	
	Fe	1.68	
Al	Al	2.60	
6061	Si	0.016	
ρ = 2.70	Fe	0.019	
	Cu	0.003	
	Mn	0.004	1
	Mg	0.027	
	Cr	0.006	
	Zn	0.007	
	Ti	0.004	
Lead	Si	0.750	
Silicate	Pb	1.065	
Glass # 2	K	0.40	50
(PPG 4966)	Ce	0.046	
ρ = 3.30	O	1.02	
$ZnBr_2$	H	0.064	
Solution	O	0.511	50
ρ = 2.37 g/cc	Zn	0.519	
	Br	1.275	
Boron Lead	Si	0.16	
Glass (PPG)	Pb	4.72	50
ρ = 5.20	B	0.24	
	O	1.05	
Lead Glass	Si	0.78	
Penberthy	Pb	4.06	50
ρ = 5.20	K	0.10	
	O	1.24	

Material	Component Elements	W_i-1 g/cc	Z cm
304L	Fe	5.43	
Stainless	Cr	1.52	
Steel	Ni	0.60	
ρ = 8.0	Co	.008	1
	Mn	0.16	
	Si	.06	
440 A	Fe	0.16	
Stainless	Cr	1.33	
Steel	Ni	0.039	
ρ = 7.8	Co	0.001	
	Mo	0.056	1
	C	0.055	
	Mn	0.078	
	Si	0.078	
Hastelloy	Ni	5.00	
"B"	Co	0.231	
ρ = 9.24	Cr	0.092	
	Mo	2.50	
	Fe	0.55	
	Si	0.092	1
	Mn	0.092	
	C	0.004	
	V	0.037	
	P	0.004	
	S	0.003	
Hastelloy	Ni	4.03	
"C"	Co	0.223	
ρ = 8.94	Cr	1.39	
	Mo	1.43	
	W	0.335	
	Fe	0.55	1
	Si	0.009	
	Mn	0.009	
	C	0.007	
	V	0.031	
	P	0.003	
	S	0.003	
Aluminum	Al	2.45	
356	Cu	0.005	
ρ = 2.68	Fe	0.013	
	Si	0.190	
	Mn	0.003	1
	Mg	0.003	
	Zn	0.005	
	Ni	0.000	
	Ti	0.005	
Aluminum	Al	2.70	
1050	Si	0.007	
ρ = 2.70	Fe	0.011	1
	Cu	0.001	
	Mn	0.001	
	Zn	0.001	

Material	Component Elements	W_i-1 b/cc	Z cm
Aluminum	Al	2.55	
2024	Si	0.014	
ρ = 2.77	Fe	0.014	
	Cu	0.12	1
	Mn	0.017	
	Mg	0.041	
	Cr	0.003	
	Zn	0.007	
Monel	Ni	5.34	
ρ = 8.90	Cu	2.94	
	Fe	0.56	
Carbon	Fe	7.59	
Steel	C	0.023	
ρ = 7.83	Mn	0.055	
	Si	0.003	
	Ni	0.039	1
	Mo	0.016	
	Cr	0.016	
	S	0.005	
	P	0.004	
	Cu	0.023	
Elgiloy	Co	3.32	
ρ = 8.31	Cr	1.66	
	Ni	1.33	
	Mo	0.582	0.0125
	Mn	.166	
	Be	.0033	
	C	.0133	
	Fe	1.23	
Almag.35	Al	2.44	
ρ = 2.66	Mg	0.186	
	Cu	0.005	
	Fe	0.008	
	Si	0.005	1
	Mn	0.003	
	Zn	0.003	
	Ti	0.005	
	Cr	0.003	

m = minutes
h = hours
d = days

Table 2. Constants for Activated Elements

Element	M	i-1	i	X_{i-1}	$\sigma_{c\ i-1}$	$E(\gamma)_i$	y_i	μ_i	$t_{1/2\ i}$
Al	26.97	Al-27	Al-28	1.00	0.23	1.78	1.00	0.048	2.3 m
Al	26.97	Al-27	Na-24	1.00	0.0006	2.76	1.0	0.038	14.8 h
Al	26.97	Al-27	Na-24	1.00	0.0006	1.38	1.0	0.054	14.8 h
As	74.91	As-75	As-76	1.00	4.2	0.60	1.00	0.080	26.6 h
As	74.91	As-75	As-76	1.00	4.2	1.20	.20	0.058	26.6 h
Ba	137.4	Ba-130	Ba-131	0.00101	10.1	0.50	1.00	0.086	11.6 d
		Ba-138	Ba-139	0.717	0.60	1.43	1.00	0.053	85 m
Be	9.013								Short
B						No γ			
Br	79.92	Br-79	Br-80	0.5054	2.9	0.037	1.0	0.30	4.5 h
Br	79.92	Br-79	Br-80	0.5054	6.5	0.620	1.0	0.079	18.5 m
Br	79.92	Br-81	Br-82	0.4946	2.6	1.31	3.0	0.056	35.9 h
Ca						No γ			
C	12.01			.0111	.0007	No γ			
Ce	140.13	Ce-142	Ce-143	.111	1.0	0.660	0.152	0.077	33 h
Ce	140.13	Ce-142	Ce-143	.111	1.0	0.356	0.73	0.10	33 h
Cr	52.01	Cr-50	Cr-51	.0431	15.0	0.323	0.098	0.103	27.8 d
Co	58.94	Co-59	Co-60	1.00	36.0	1.2	1.00	0.058	5.27 y
Cb	92.91					No γ			
Cu	63.57	Cu-63	Cu-64	.691	4.1	1.35	0.005	0.055	12.82 h
		Cu-65	Cu-66	.309	2.0	1.044	0.090	0.062	5.15 m
H						No γ			
Fe	55.85	Fe-58	Fe-59	0.0031	0.98	1.10	0.57	0.060	45.1 d
Fe	55.85	Fe-58	Fe-59	0.0031	0.98	1.29	0.43	0.056	45.1 d
Fe	55.85	Fe-54	Mn-54	0.0584	0.056	0.835	1.0	0.069	300 d
Pb						No γ			
Mg	24.32	Mg-26	Mg-27	.1129	0.027	1.02	1.0	0.063	9.45 m
Mg	24.32	Mg-24	Na-24	0.787	0.001	2.76	1.0	0.038	14.8 h
Mg	24.32	Mg-24	Na-24	0.787	0.001	1.38	1.0	0.054	14.8 h
Mn	54.93	Mn-55	Mn-56	1.00	13.3	0.845	1.0	0.068	2.58 h
Mn	54.93	Mn-55	Mn-56	1.00	13.3	2.13	1.0	0.043	2.58 h
Mo	95.95	Mo-98	Mo-99	.2375	0.45	0.78	0.25	0.071	67 h
Mo		Mo-100	Mo-101	0.0952	0.20	0.96	1.00	0.064	14.6 m
Ni	58.69	Ni-64	Ni-65	0.0116	1.6	1.5	1.00	0.052	2.56 h
Ni	58.69	Ni-58	Co-58	0.678	0.061	0.81	0.14	0.070	72 d
Ni	58.69	Ni-58	Co-58	0.678	0.061	1.62	0.02	0.050	72 d
O									Short
P	30.98	P-31	Si-31	1.00	0.019	1.26	0.0007	0.056	2.65 h
K	39.10	K-41	K-42	.0691	1.17	1.53	0.25	0.051	12.47 h
Si	28.06	Si-30	Si-31	0.0312	0.11	1.26	0.0007	0.057	2.65 h
Na	23.0	Na-23	Na-24	1.00	0.53	2.76	1.0	0.038	15.0 h
Na	23.0	Na-23	Na-24	1.00	0.53	1.38	1.0	0.054	15.0 h
S	32.06	S-34	Si-31	0.042	0.003	1.26	0.0007	0.057	2.65 h
Ta	180.9	Ta-181	Ta-182	1.00	19.0	1.12	0.12	0.060	112 d
Sn	118.7	Sn-112	Sn-113	0.0095	1.3	.256	1.0	0.113	115 d
Sn	118.7	Sn-122	Sn-123	0.0972	0.16	.153	1.0	0.140	40 m
Sn	118.7	Sn-124	Sn-125	0.0598	0.20	1.97	1.0	0.045	9.5 d
Ti	47.90	Ti-50	Ti-51	0.0525	0.14	0.32	0.10	0.102	5.79 m
W	183.9	W-186	W-187	0.284	34	0.70	1.0	0.075	24.0 h
V	50.96	V-51	Sc-48	0.9976	0.00008	1.33	3.0	0.055	1.83 d
Zn	65.38	Zn-64	Zn-65	0.469	0.40	1.11	0.46	0.062	245 d
Zn	65.38	Zn-68	Zn-69	0.18	0.097	0.438	1.0	0.092	13.8 h

(Fe cross sections used), and B = 0.0, 0.0005, 0.0050 and 0.050. The flux in the vicinity of a 100-liter sphere containing a solution emitting 10^{14} neutrons/sec was evaluated for a bare sphere and for a sphere coated with a 20-mil sheet of cadmium.

4.0 RESULTS AND CONCLUSIONS

4.1 Neutron Flux

The fast (fission energy) and thermal neutron flux in a cell and natural boron-magnetite concrete wall for a point S.F. neutron source of 10^{14} neutrons/sec located four feet from the inside cell wall is shown in Fig. 1. The values of flux for other sources located in this position may be evaluated through the use of a direct proportion. The effect of fast activation thresholds may be evaluated by assuming that inside the cell and at the concrete wall the 3.0-10, 1.4-3.0, 0.9-1.4, 0.4-0.9, and 0.1-0.4 mev fluxes are 20.4, 34.4, 16.8, 18.0 and 9.0 percent of the fast flux, respectively. The thermal flux decreases considerably with increasing boron content in the concrete wall; a cross-plot of these data indicates that boron densities of 6.0 and 24 lbs/cu yd decreases the thermal flux in the cell by approximately a factor of 10 and 100, respectively. Since the thermal flux at the surface of the boron-free concrete wall is a factor of 3.8 lower than the fast flux 2.6 and 13 lbs/cu yd of boron in the concrete is sufficient to lower the thermal flux factors of 10 and 100 below the fast flux.

The fast (>0.1 mev), intermediate, and thermal flux at the surface of a 100 liter sphere containing a homogeneous water solution of a source of 10^{14} neutrons/sec is 1.5×10^9, 1.6×10^9, and 0.86×10^9 neutrons/sec-cm^2, respectively. The thermal flux is lowered by approximately a factor of 400 by coating the sphere with 20 mils of cadmium. Boron in the concrete must be used in conjunction with a cadmium coating on the sphere if the thermal flux in the cell is to be lowered; this effect is shown in Table 3.

It becomes infeasible to lower the thermal flux to levels below which the thermal activation is approximately equal to the fast activation. The relative thermal and fast activation in materials of construction that will be abundant in the Transuranium Laboratory is illustrated in Table 4. The relative activation in these materials

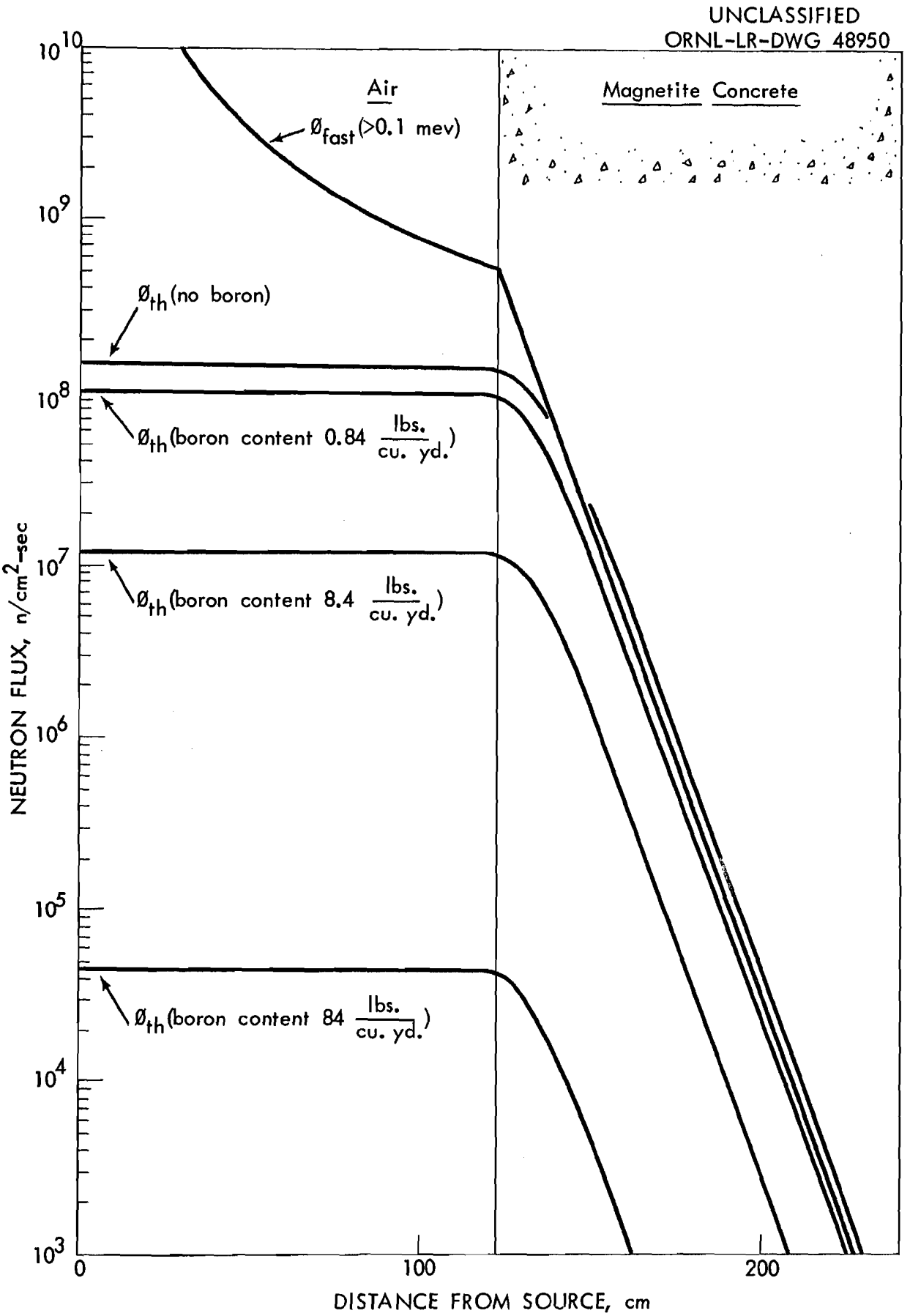

Fig. 1. The fast and thermal neutron flux in a cell and boron-magnetite wall for a 10^{14} n/sec fission source located four feet from the wall.

Table 3. The Effect of Concrete Boron Content and Cd Tank Lining on the Flux in the Vicinity of a 100-liter Tank Containing a Solution Source of 10^{14} neutrons/sec.

Cadmium Thickness on Tank, mils	Boron Density in Concrete lbs/cu yd	Fast Flux (>0.1 mev)		Thermal Flux	
		At Surface of Tank	At Concrete Wall	At Surface of Tank	In Cell
0	0.0	1.5×10^9	10^8	8.6×10^8	$\sim 6 \times 10^7$
0	2.6	1.5×10^9	10^8	8.6×10^8	$\sim 6 \times 10^7$
0	13	1.5×10^9	10^8	8.6×10^8	$\sim 6 \times 10^7$
20	0.0	1.5×10^9	10^8	$\sim 10^8$	2.6×10^7
20	2.6	1.5×10^9	10^8	$\sim 10^7$	$\sim 10^7$
20	13	1.5×10^9	10^8	$\sim 10^6$	$\sim 10^6$

Table 4. The Relative Activation of Construction Materials by A Fast and Thermal Neutron Flux of 10^{10} neutrons/sec-cm^2

Material	Irrad. Time at Flux = 10^{10}, days	Cooling Time, days	Slab Thickness, cm	Dose Rate at Surface of Slab, mr/hr	
				Thermal Flux	Fast (>0.1 mev) Flux
Carbon	10	1	1	795	46
Steel	10	10	1	322	45
	10	100	1	81	36
	100	1	1	2464	410
	100	10	1	1777	400
	100	100	1	451	320
Magnetite	100	1	≥ 25	2121	549
Concrete	100	10	≥ 25	1818	344
	100	100	≥ 25	453	280
304L	100	1	1	6205	545
S.Steel	100	10	1	4508	518
	100	100	1	1577	326

indicates that it is probably not feasible to add boron or cadmium in excess of that required to lower the thermal flux in the cell more than an order of magnitude below the fast flux; this result could be achieved by coating tanks such as that described in the previous paragraph with approximately 15 mils of cadmium and adding approximately 2.6 lbs/cu yd of boron to the concrete.

The maximum and most probable values of neutron source strength and neutron flux that will occur at various locations in the Transuranium Laboratory are tabulated in Table 5. A prolonged fast flux of 10^8 and thermal flux of 10^8 or 10^7, depending on the thermal neutron poisoning, could occur in cell 3, 4, 5 pits. Similar fluxes could occur in cell 6, 7, 8 cubicle for periods of 1-10 days.

4.2 Activation Calculations

The results of the activation calculations for the materials that were evaluated are plotted in Figs. 2-45. Figs. 2-39 were calculated assuming irradiation by simultaneous fast (>0.1 mev) and thermal fluxes of 10^{10}, in general, the fast activation contribution constitutes in the order of 10% of the total for the decay times shown. Figures 40-45 were calculated assuming only a fast flux of 10^{10}. The type of radiation that constitutes the controlling activity at various decay times may be evaluated by examining the slope of the curves and the properties of materials and isotopes given in Tables 1 and 2. The dose rates for configurations other than slabs may be evaluated using the same procedure or a geometrical transformation. The energy density,

$$\sum_{i=1}^{i=n} \sum_{j=1}^{j=m} A_i(T,t) y_{ij} E_{ij},$$

in mev/sec-cc may be obtained using the slab dose curves and equations (2) and (3) in Section 3.0. For all of the metal materials and 2.7 density non-browning glass the energy density is simply 1160 $D(T,t)/Z$. For other glasses, zinc bromide solution, and magnetite concrete, the energy density is 1160 $D(T,t)\ \rho\mu_{avg}$ where μ_{avg} must be determined from inspection of the slope of the curve at T,t and the properties of the materials and isotopes.

Table 5. The Magnitude of Fast and Thermal Fluxes that May Occur In Transuranium Facility Cells

Location	Condition	Neutron Source Strength, Neutrons/second	Exposure Time, days	Approximate Fast Flux Near Walls & Manipulators	Thermal Flux in Cell: No Boron or Cadmium	Thermal Flux in Cell: Concrete Contains 2.6 lbs/cu yd Boron "HOT" Tanks Coated with Cd
Cell 1-2	Maximum	10^{11}**	100	5×10^5	1.4×10^5	5×10^4
	Probable	10^9 **	1000	5×10^3	1.4×10^3	5×10^2
Cell 3,4,5	Maximum	10^{14}**	1000	10^8	6×10^7	10^7
Pit	Probable	10^{13}**	1000	10^7	6×10^6	10^6
Cell 3,4,5	Maximum	10^{13}**	1	5×10^7	1.4×10^7	5×10^6
Cubicle	Probable	10^{11}**	10	5×10^5	1.4×10^5	5×10^4
Cell 6,7,8	Maximum	2×10^{13}**	10	10^8	2.6×10^7	10^7
Cubicle	Probable	2×10^{13}**	1	10^8	2.6×10^7	10^7
Cell 9,10	Maximum	10^{11}**	100	5×10^5	1.4×10^5	5×10^4
Cubicle	Probable	10^{11}**	10	5×10^5	1.4×10^5	5×10^4

**As small volume of solution or dry (no water self-shielding considered)

* As solution in tank (water self-shielding considered)

4.2.1 Concrete Walls

The data in Table 5, Figs. 7 and 41, and consideration of the cell geometry allows prediction of the dose rates that will occur in Transuranium cells due to activation of the concrete. The gamma flux in pits which might be exposed to fast and thermal neutron fluxes of $\sim 10^8$ for 1000 days would be equivalent to 50-200 mr/hr 1-100 days subsequent to exposure. If boron is added to suppress the thermal neutron flux the gamma flux would be lowered by a factor of 2-5. The data in ORNL-1371[3] indicates that ordinary concrete is a factor of 2-3 less radioactive than magnetite concrete for flux exposure and decay times of interest. The exposure of unborated magnetite walls to fluxes of 10^8 for 1-10 days such as could occur in Cell 6, 7, 8 cubicles would result in gamma fluxes in the cells equivalent to 1-20 mr/hr for decay times of 1-100 days. A 10^{14} neutron source located 2 ft from an unborated magnetite wall for 1 day would cause fast and thermal fluxes at the wall of approximately 10^9 and would cause a wall "hot spot" surveying 30 mr/hr one day after exposure.

4.2.2 Windows

Oil-filled lead glass windows such as those being considered for use in the Transuranium Laboratory when exposed to fast and thermal neutron fluxes of 10^9 for 1-1000 days would survey approximately 30,000, 10, and 0.1 mr/hr after decay times of 1, 10, and 100 days, respectively. The sodium in the glass contributes the bulk of the activity and the oil is not significantly activated. The dose rate would, of course, be proportionally lower for the 10^7-10^8 fluxes which will be more likely to occur in the window.

Zinc bromide windows become activated to a considerable extent. Windows exposed to neutron sources such as will be present in the Transuranium Laboratory would have to be compartmentalized to prevent radioactive solution from circulating to the operating face and causing dose rates in the order of several rem per hour.

4.2.3 Manipulators

A CRL Model D master-slave manipulator located in cubicles which could contain several hundred mg of Cf^{252}-Cf^{254} for up to 10 days would be exposed to fluxes of the order of 10^8. The dose rate at the surface of the stainless steel arm and carbon steel through-tube resulting from such an exposure would be approximately 2 R/hr, 10 mr/hr, and 1 mr/hr for decay times of 1 hour, 1 day, and 100 days, respectively. The Elgiloy tapes would survey approximately

50 mr/hr after 1 hour and would remain at approximately 5 mr/hr for decay times of 1-1000 days. These data and the presently envisaged plans for operation of the Transuranium Laboratory indicate a very high probability that at a given time none of the manipulators in the Laboratory would survey greater than 10 mr/hr. Personnel could only be exposed to high dose rates in the rare event that it was necessary to contact a manipulator which had been exposed to a maximum source after less than one day decay time.

4.2.4 Process Vessels and Structural Materials

Typical process vessels and structural materials that will become activated are the dissolver, mixer-settlers, Cf^{252}-Cf^{254} storage tank, which are assumed to be constructed of Hastelloy "B" or "C", and 304L stainless steel equipment racks. The dissolver, which could be exposed to sources of 5×10^{13} n/sec for 1-2 days, would survey 35 and 25 mr/hr after 10 and 100 days decay time, respectively. Mixer-setters, which could be exposed to fluxes in the order of 5×10^{8} n/cm^{2}-sec for periods up to 10 days, would survey 190 and 155 mr/hr after 10 and 100 days, respectively. The californium storage tank, which could be used to store Cf^{252}-Cf^{254} solutions for periods of a year or longer would survey 10-20 R/hr for decay times of 1-1000 days. Stainless steel equipment racks which could be exposed to fast and thermal fluxes of 10^{8} for 1000 days would survey 100-200 mr/hr for decay times of 1-100 days; the degree of activation in these components could be lowered almost a factor of 10 by coating californium storage vessels with Cd and including boron in the concrete.

Jere P. Nichols

JPN/nr

J. P. Nichols

REFERENCES

1. Blomeke and Todd, "Uranium-235 Fission Product Production as a Function of Thermal Neutron Flux, Irradiation Time, and Decay Time," ORNL-2127, (1957).
2. W. H Sullivan, "Trilinear Chart of Nuclides," (1957).
3. C. D. Bopp, "Gamma Radiation Induced in Engineering Materials," ORNL-1371 (1953).
4. B. T. Price, et al, "Radiation Shielding," Pergamon Press (1957).

ORNL-LR-Dwg. 59557
Unclassified

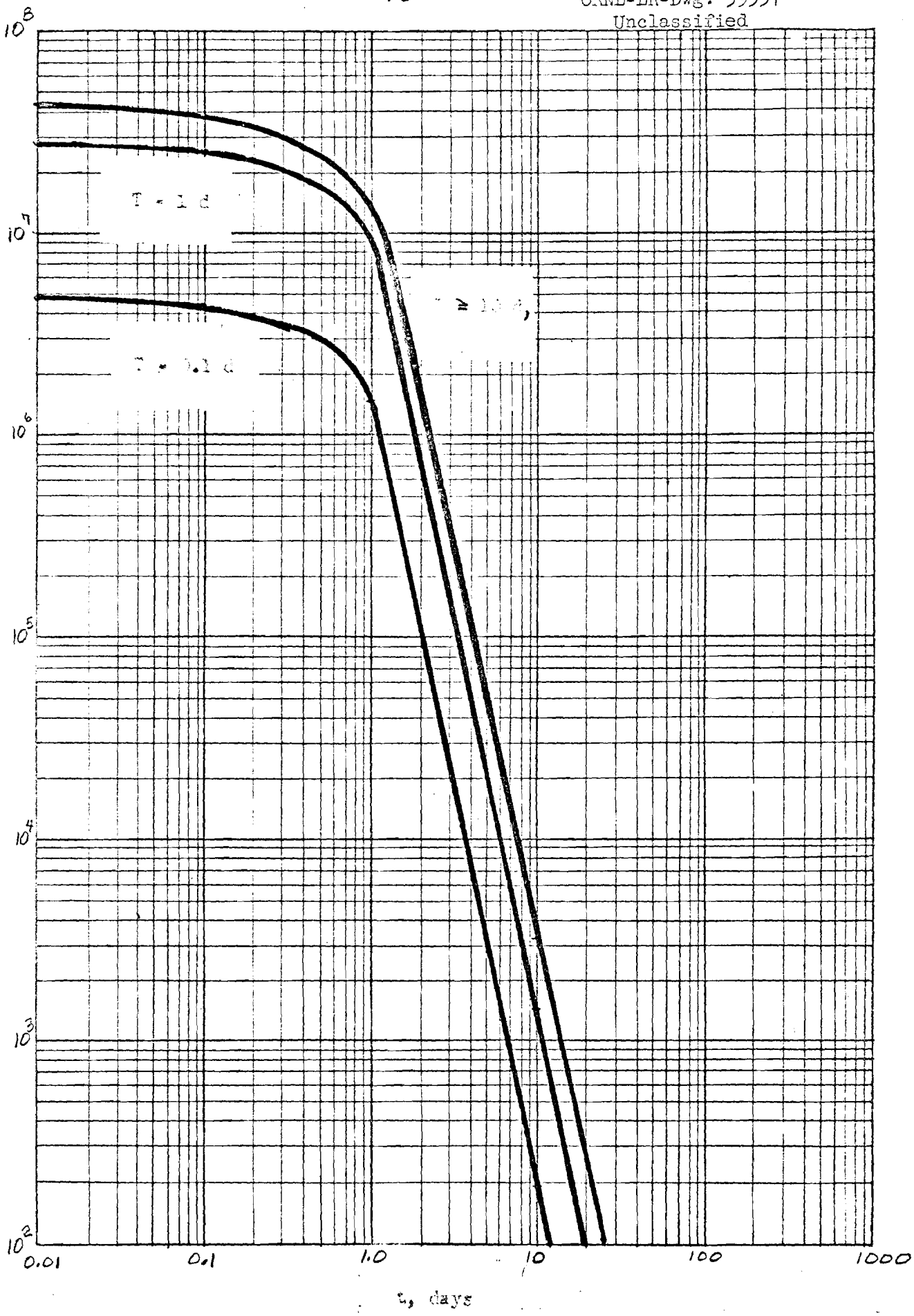

FIGURE 2 ADDITIVATION GAMMA ACTIVITY AS A FUNCTION OF IRRADIATION TIME, T, AND DECAY TIME, t.

ORNL-LR-Dwg. 59558
Unclassified

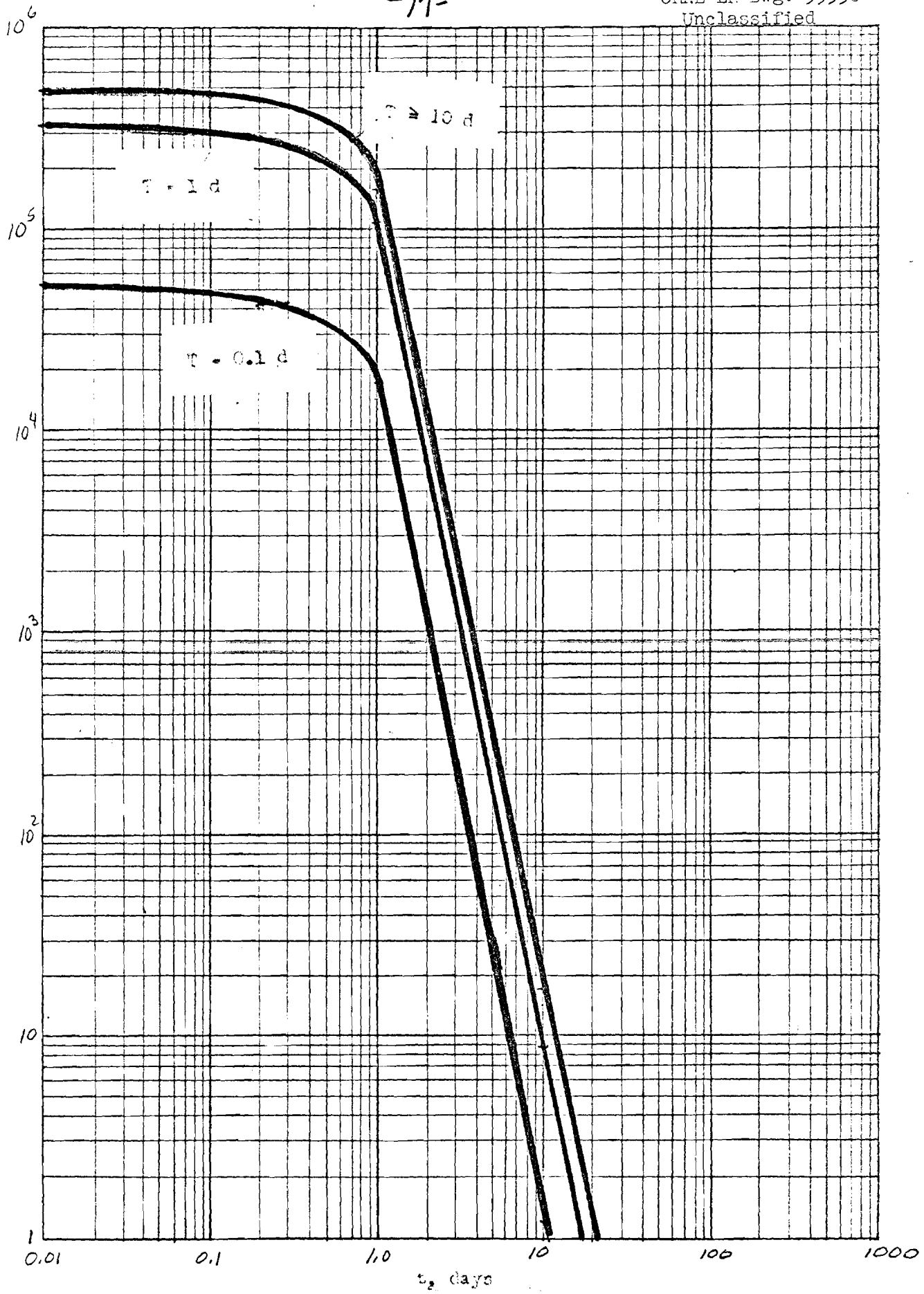

FIGURE 3 ACTIVATION GAMMA DOSE RATE AT THE SURFACE OF A SLAB AS A FUNCTION OF IRRADIATION TIME, T, AND DECAY TIME, t.

MATERIAL: LEAD SILICATE GLASS # 1

ORNL-LR-Dwg. 59559
Unclassified

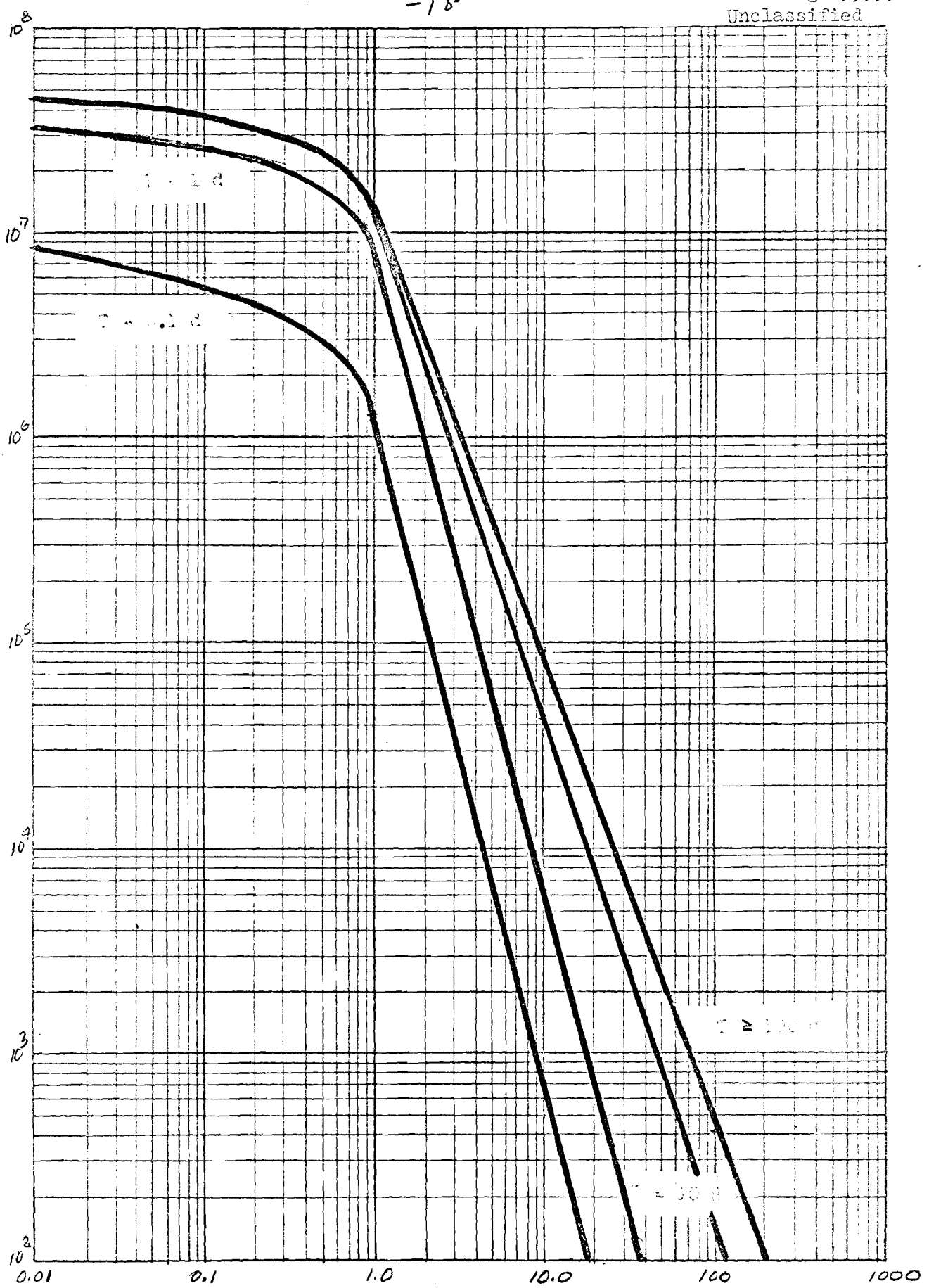

4 [illegible] GAMMA ACTIVITY AS A FUNCTION OF [illegible]

27 DENSITY NONBROWNING GLASS (PPG 6790)

ORNL-LR-Dwg. 59560
Unclassified

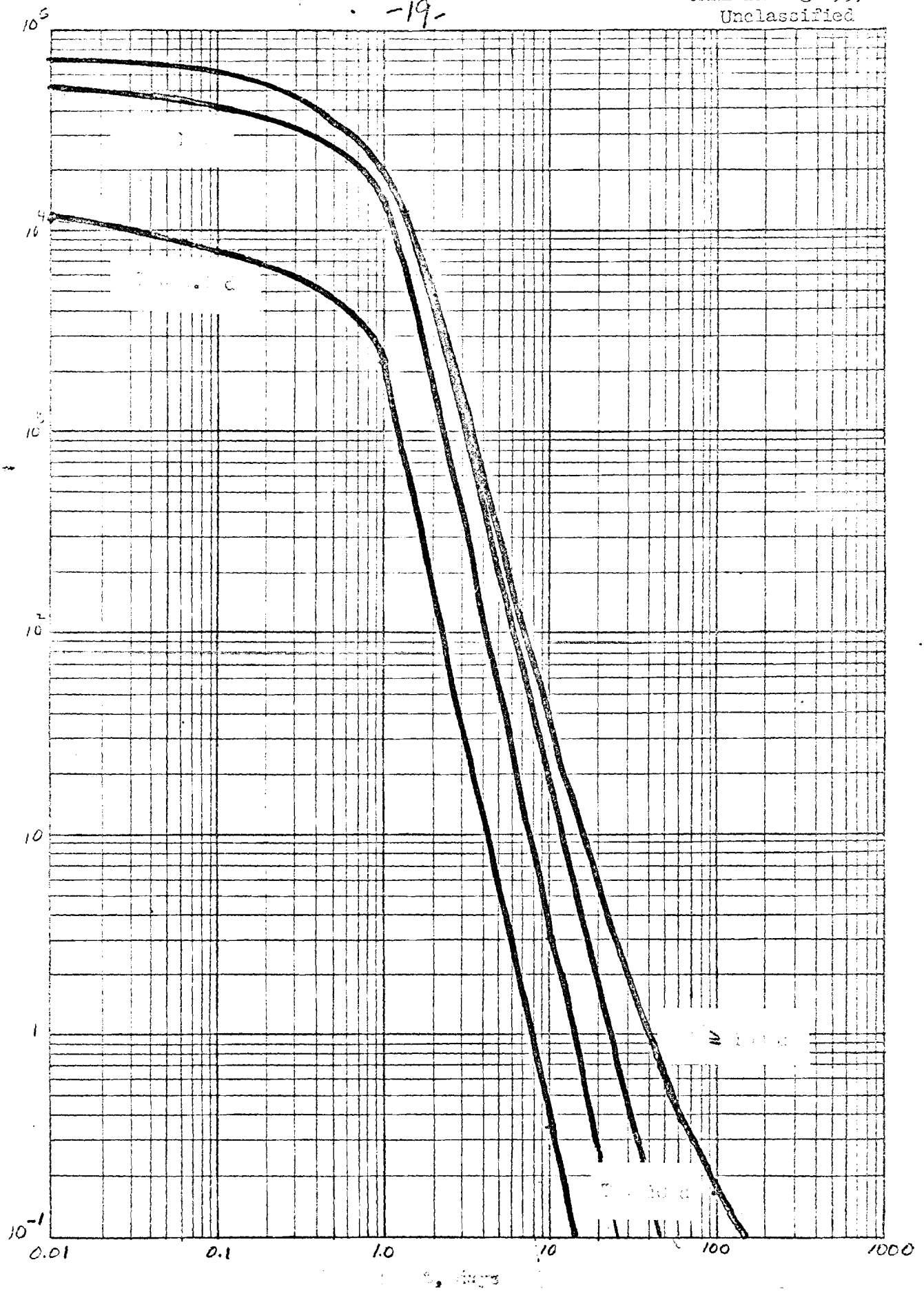

FIG. 5 [illegible]

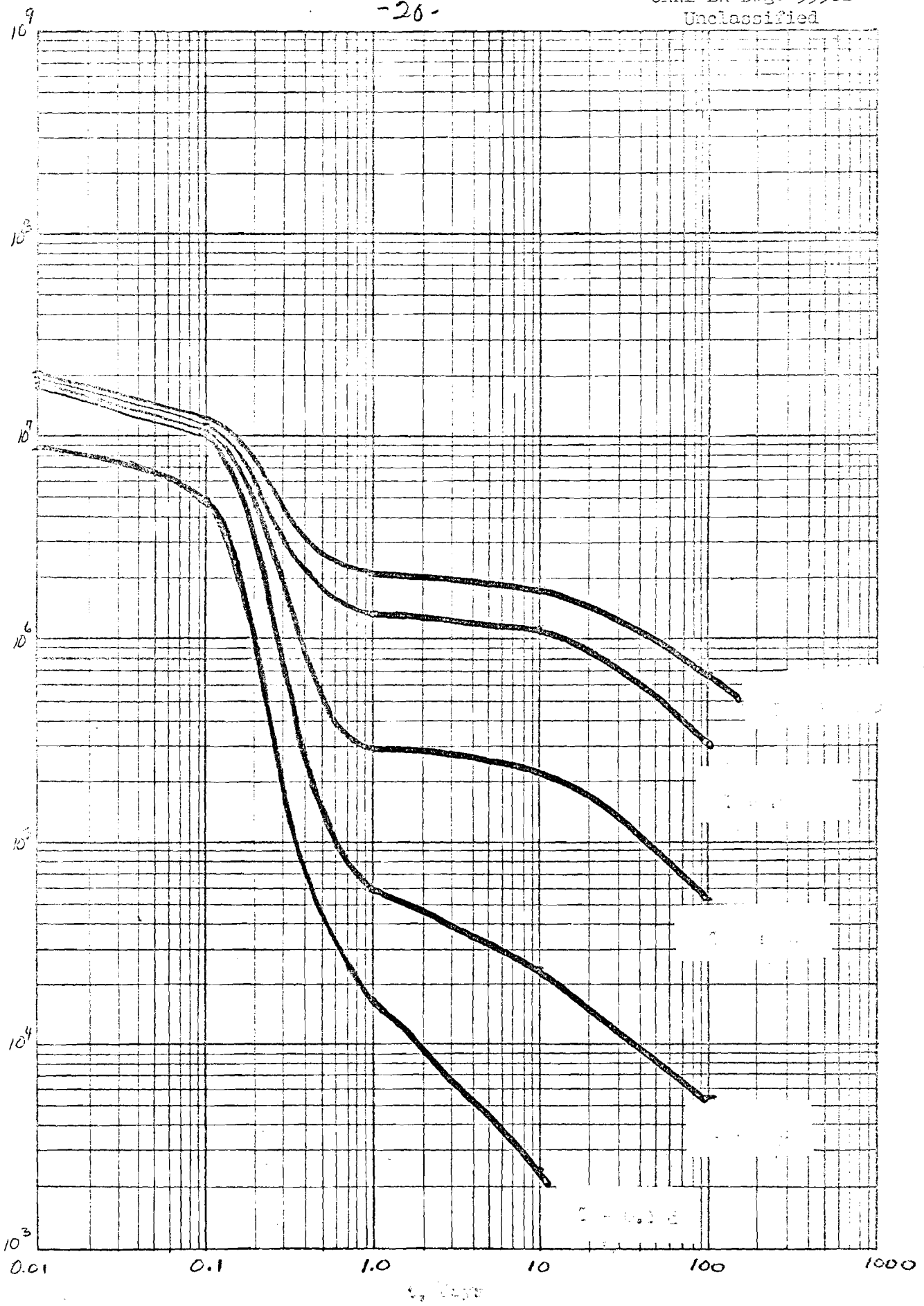

FIGURE 6 ACTIVATION [illegible] AS A FUNCTION OF IRRADIATION [illegible] AND DECAY [illegible]

ORNL-LR-Dwg. 59562
Unclassified

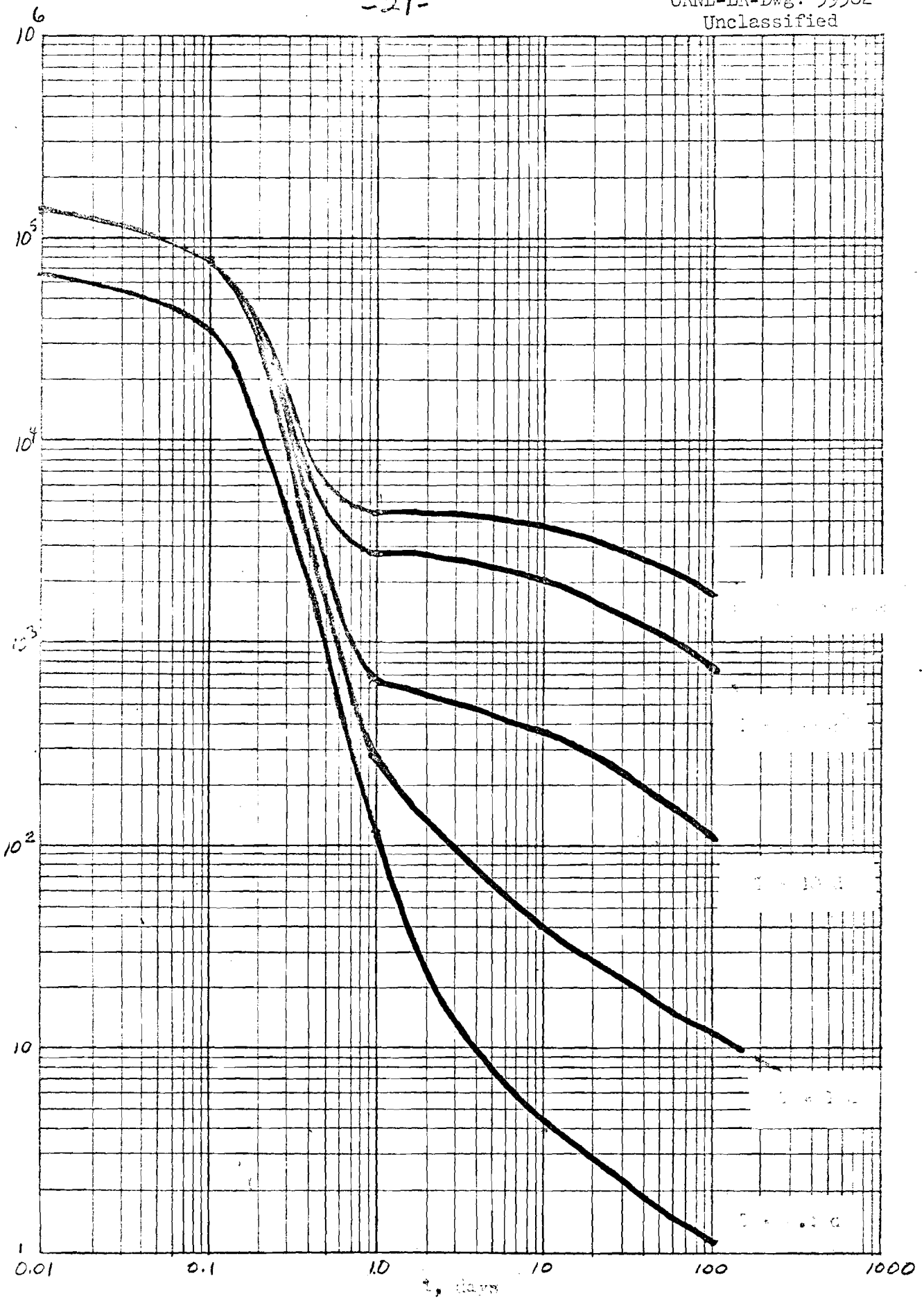

FIGURE 7 ACTIVATION GAMMA DOSE RATE AT THE SURFACE OF A SLAB AS A FUNCTION OF IRRADIATION TIME, T, AND DECAY TIME, t.

MATERIAL: MAGNETITE CONCRETE

ORNL-LR-Dwg. 59563
Unclassified

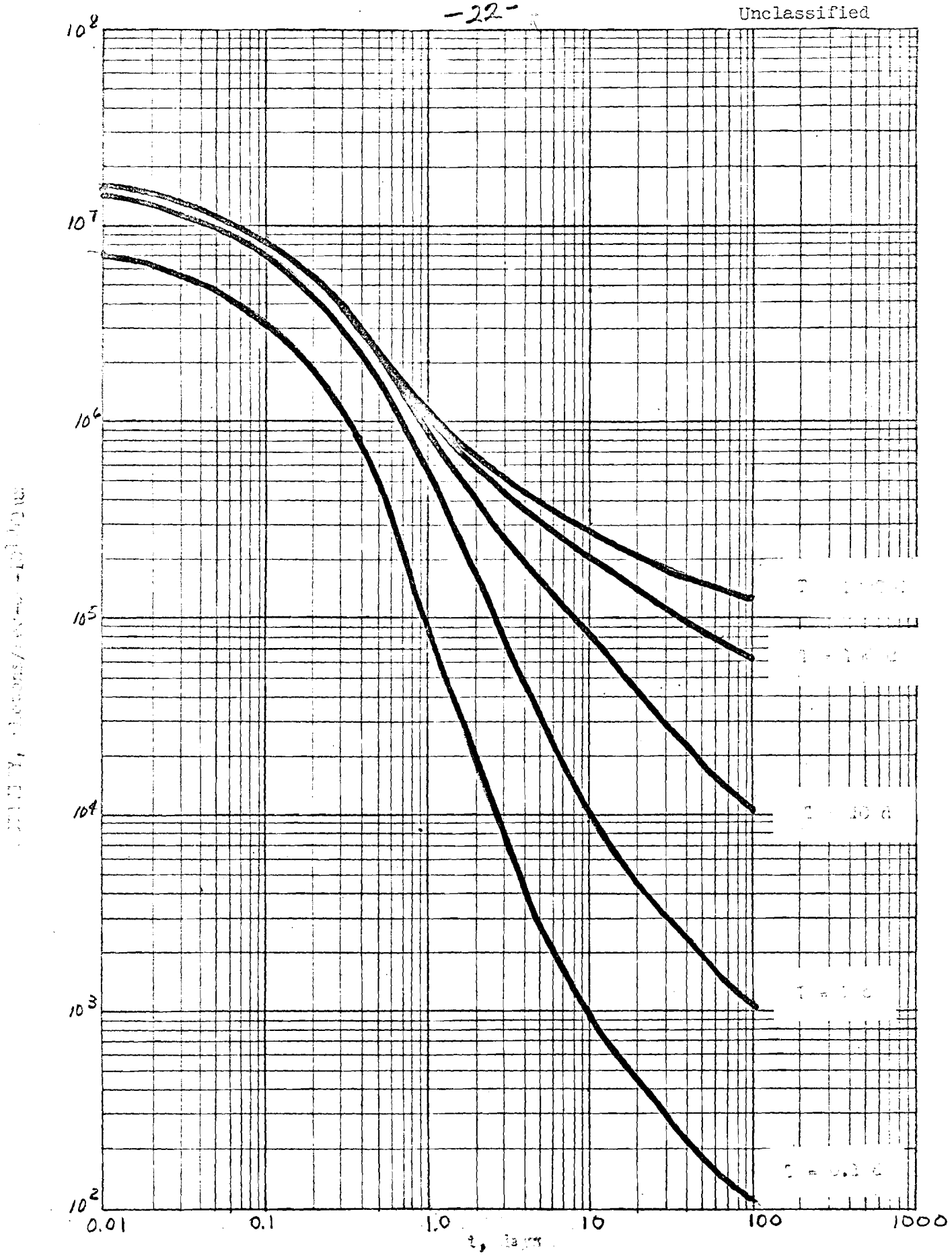

FIGURE 8 ACTIVATION GAMMA ACTIVITY AS A FUNCTION OF IRRADIATION TIME, T, AND DECAY TIME, t.

ORNL-LR-Dwg. 59564
Unclassified

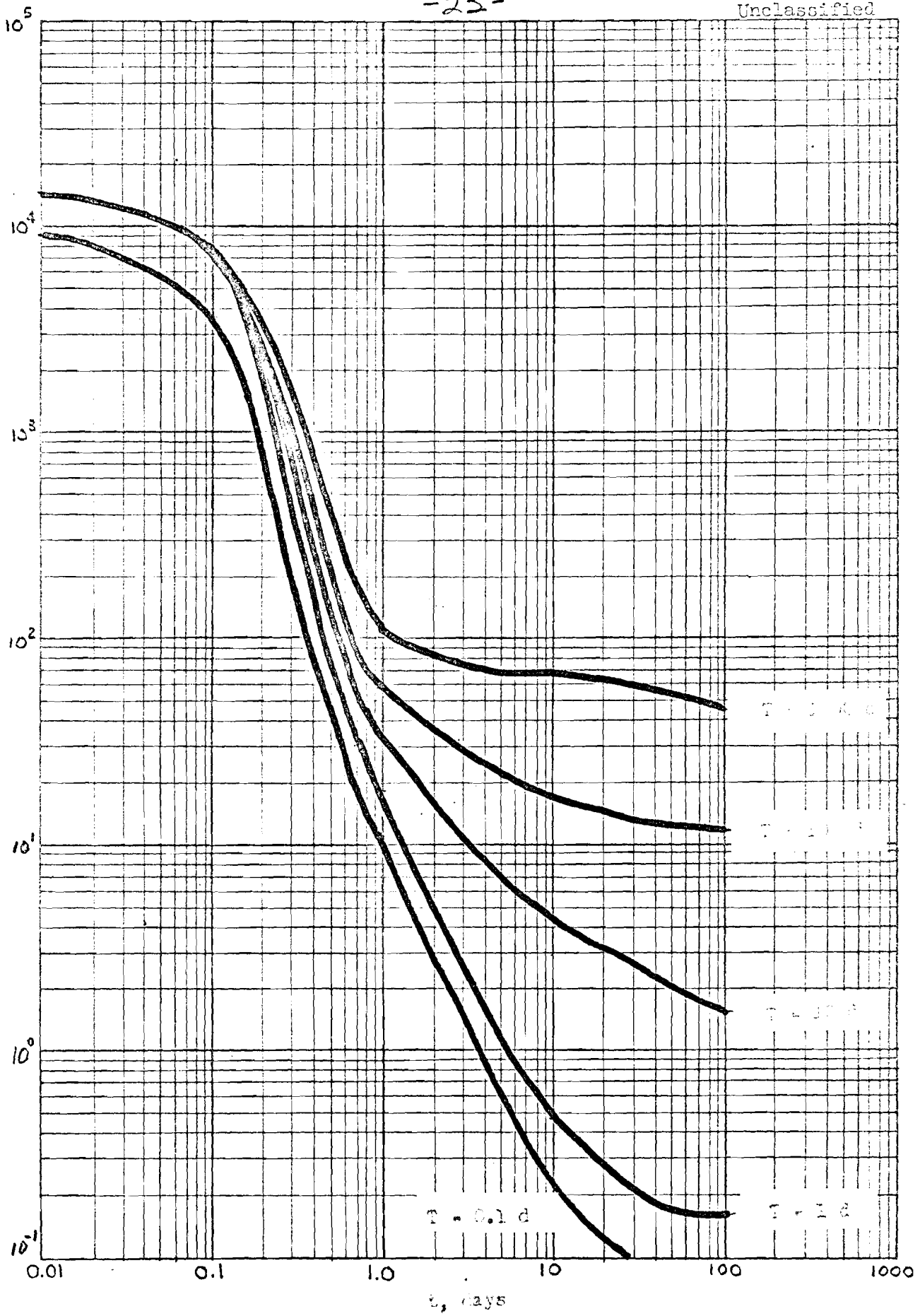

FIGURE 9 [illegible] DOSE RATE AT THE SURFACE OF A SLAB AS A FUNCTION OF IRRADIATION TIME, T, AND DECAY TIME, t.

MATERIAL: ALUMINUM 6061

ORNL-LR-Dwg. 59565
Unclassified

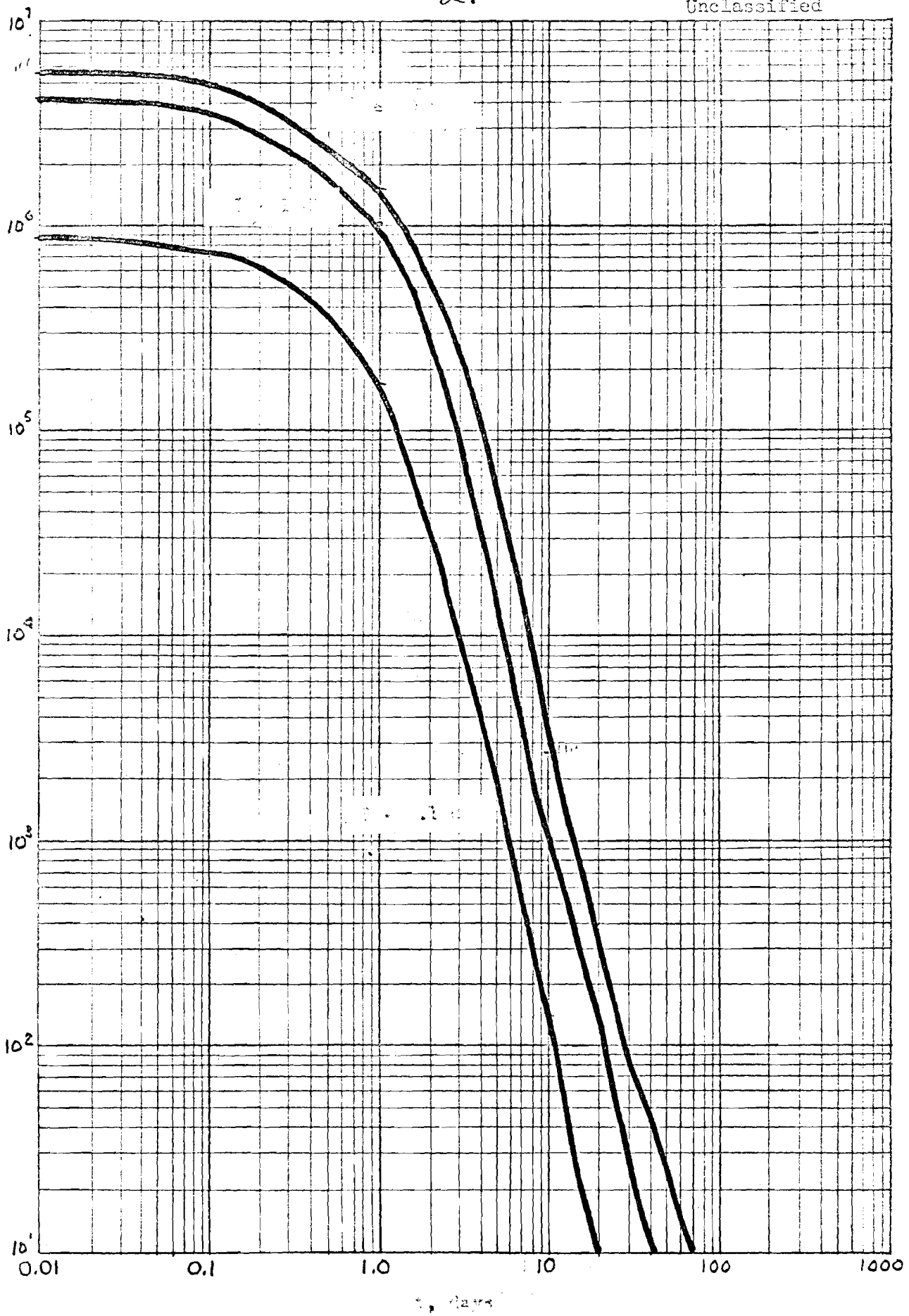

FIGURE 10 ACTIVATION GAMMA FOR THE AS A FUNCTION OF IRRADIATING TIME, [illegible] AND DECAY TIME, [illegible].

ORNL-LR-Dwg. 59566
Unclassified

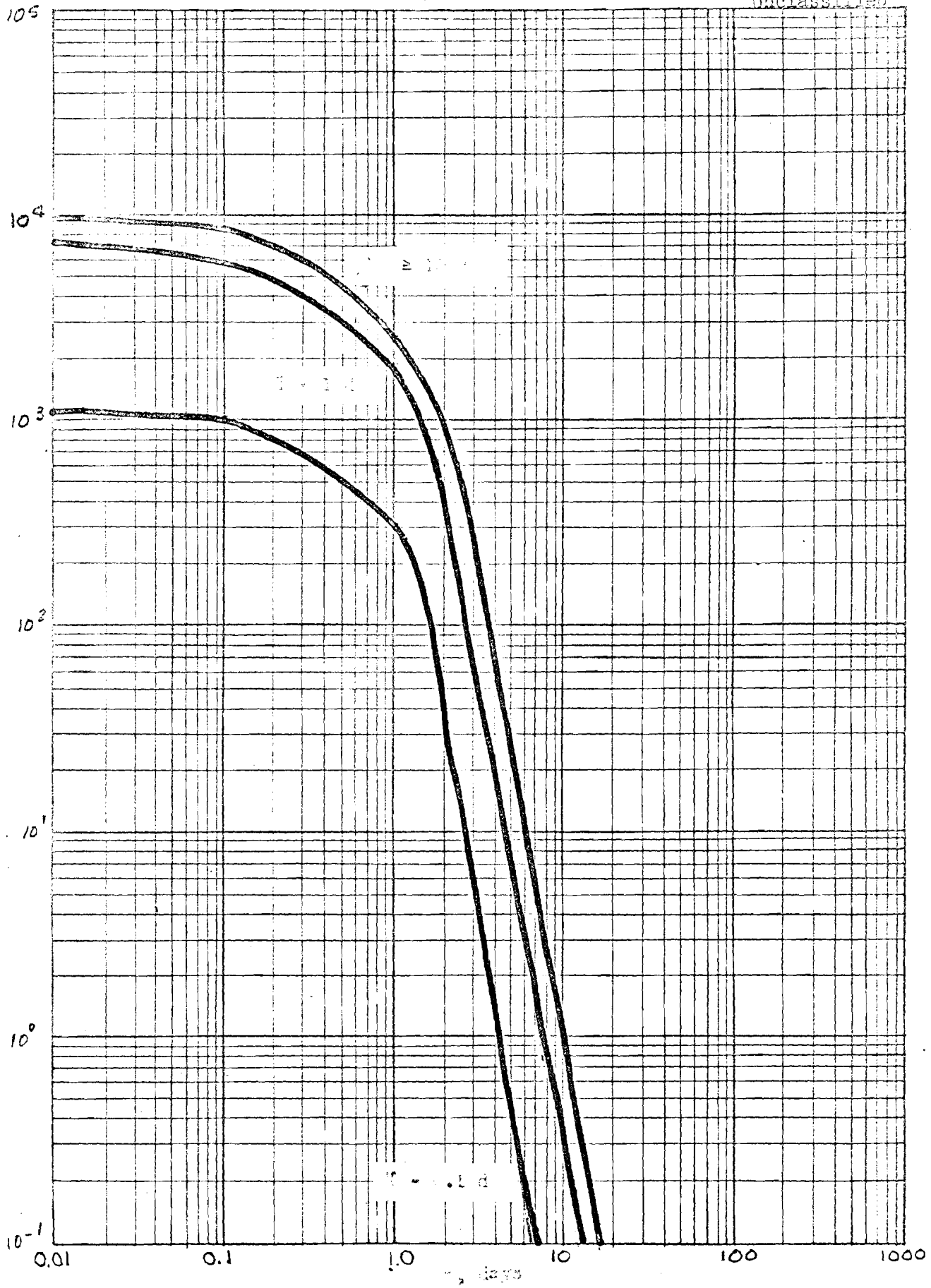

FIGURE 11 [illegible] LEAD SILICATE GLASS #2

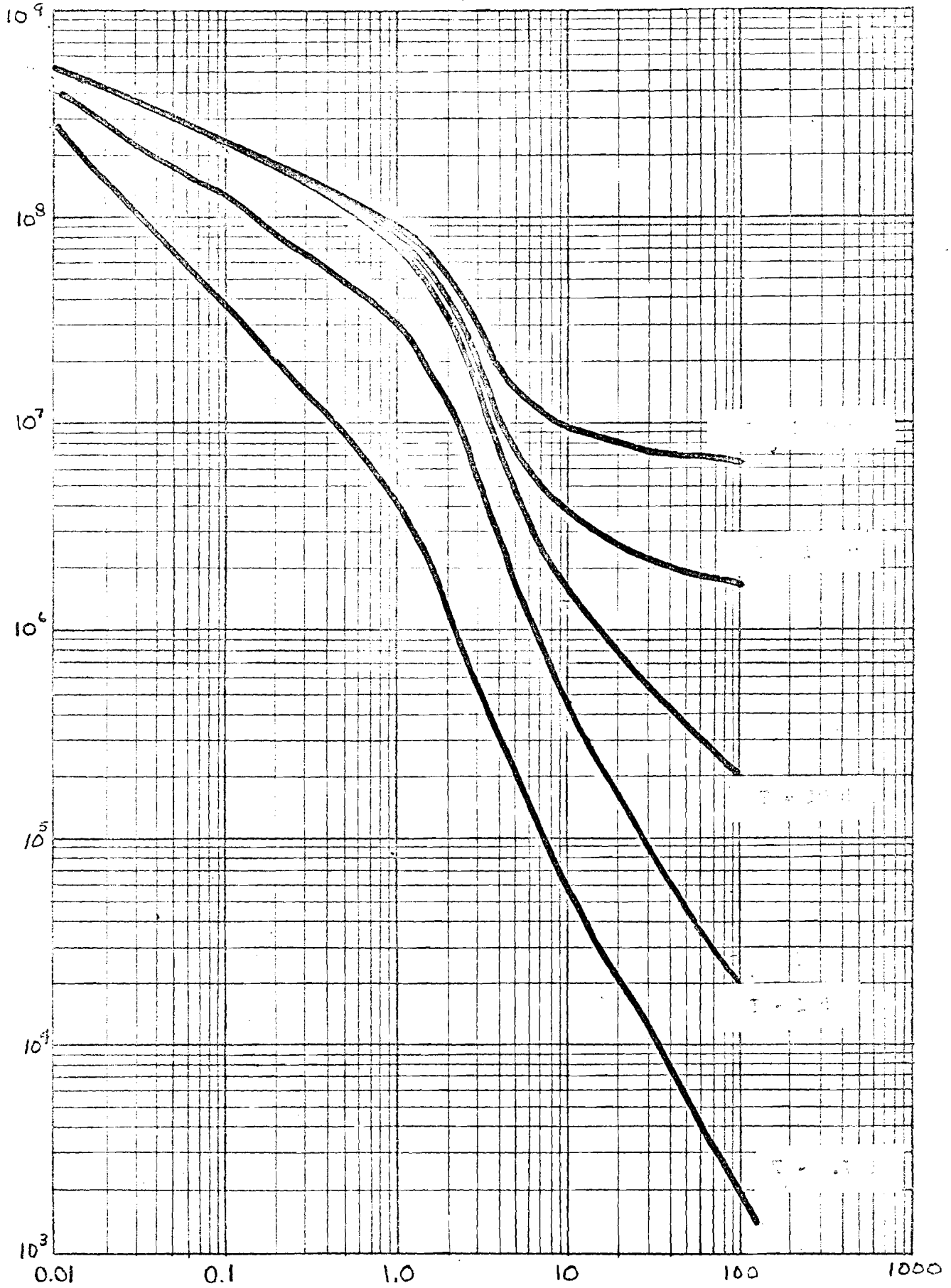

FIG. 12 ADSORPTION [illegible] AS A FUNCTION OF IRRADIATION [illegible] AND [illegible] TIME

ORNL-LR-Dwg. 59568
Unclassified

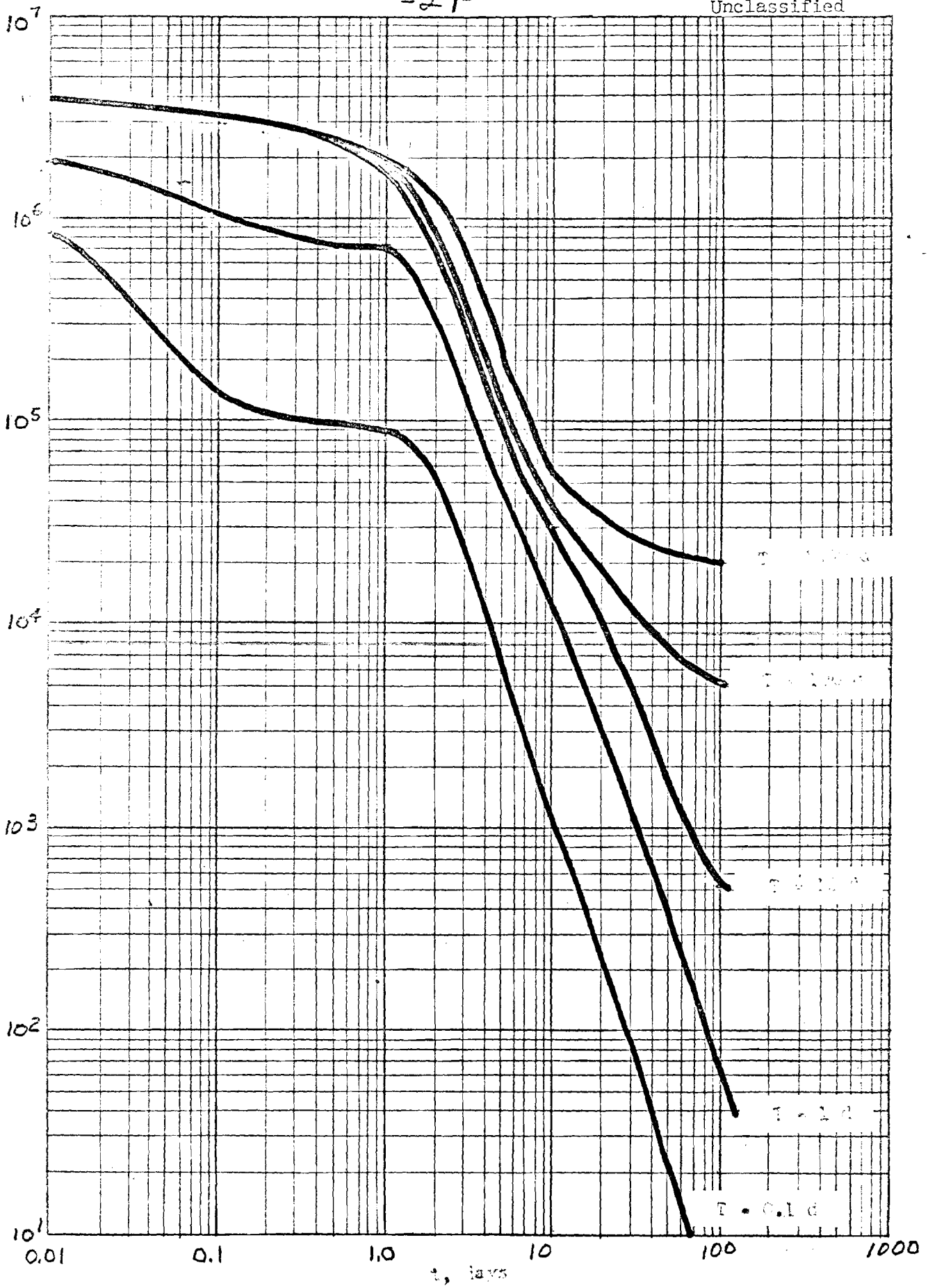

FIGURE 13 ACTIVATION RATE DEVELOPED AT THE SURFACE OF A SLAB AS A FUNCTION OF IRRADIATION TIME, T, AND DECAY TIME, t.

MATERIAL: Z_n-Br- SOLUTION

ORNL-LR-Dwg. 59569
Unclassified

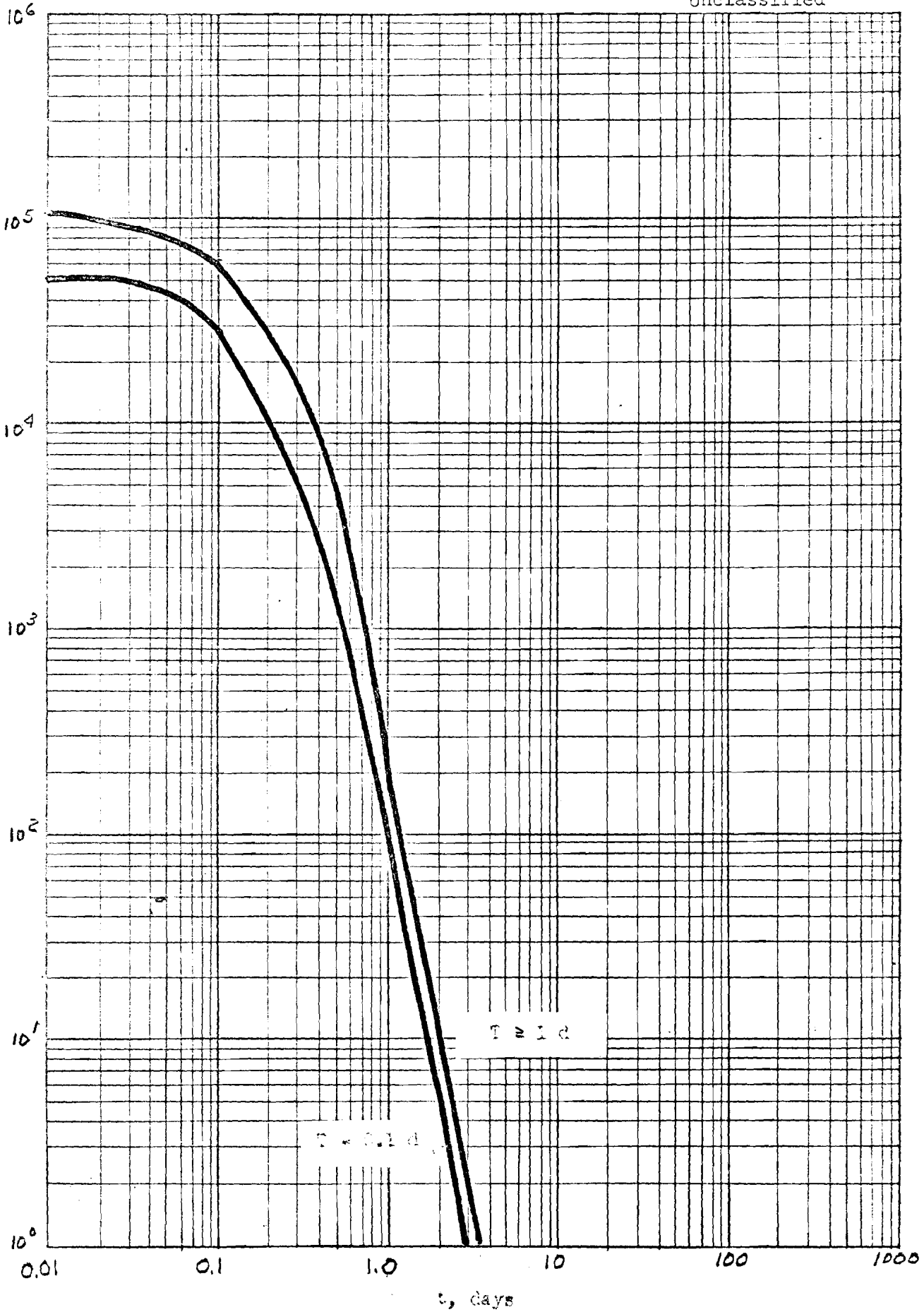

FIGURE 14 ACTIVATION GAMMA ACTIVITY AS A FUNCTION OF IRRADIATION TIME, T, AND DECAY TIME, t

ORNL-LR-Dwg. 59570
Unclassified

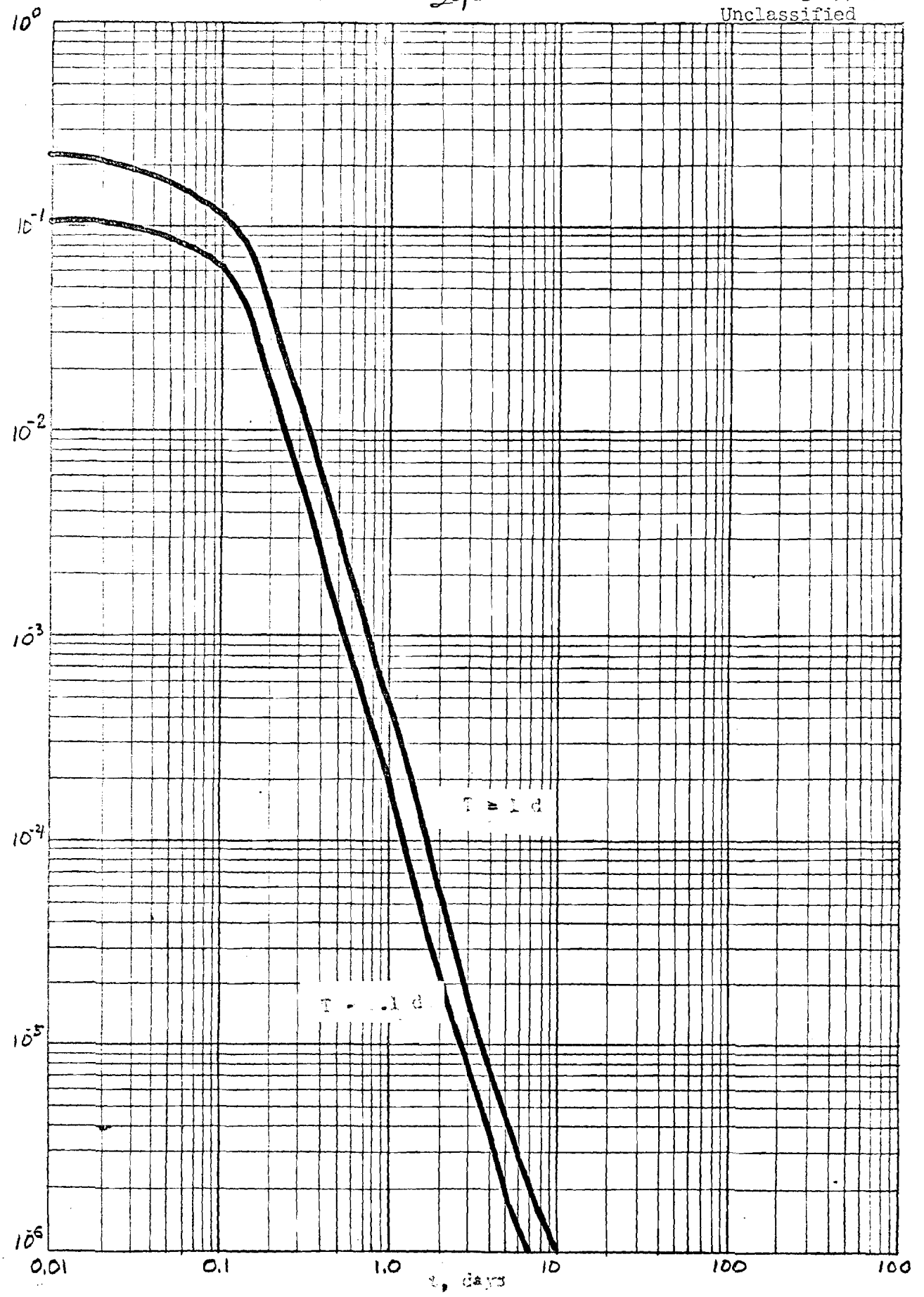

FIGURE 15 ACTIVATION GAMMA DOSE RATE AT THE SURFACE OF A SLAB AS A FUNCTION OF IRRADIATION TIME, T, AND DECAY TIME, t.

MATERIAL: BORON LEAD GLASS (PDG)

ORNL-LR-Dwg. 59571
Unclassified

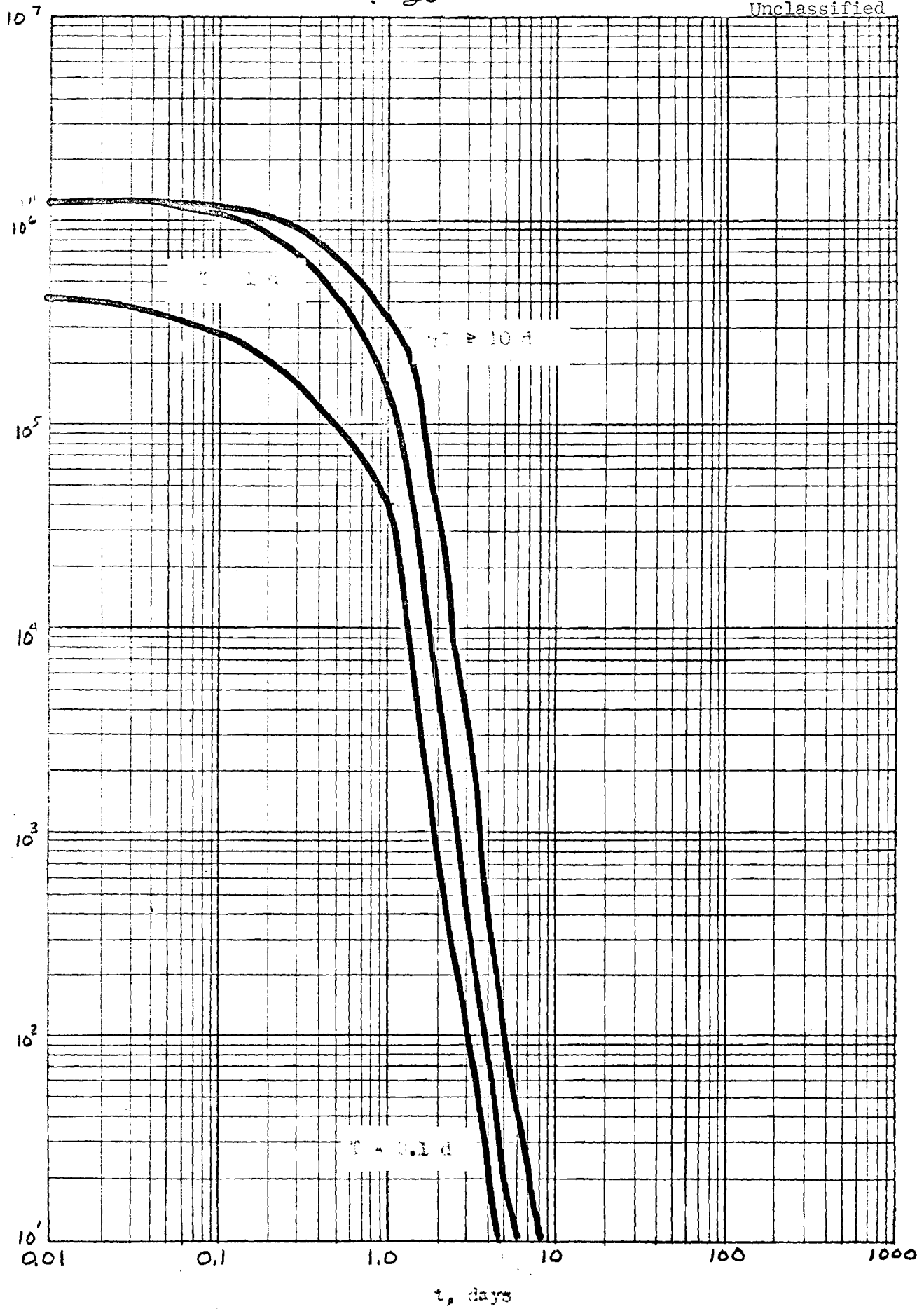

FIGURE 16 ACTIVATION GAMMA ACTIVITY AS A FUNCTION OF IRRADIATION TIME, T, AND DECAY TIME, t.

ORNL-LR-Dwg. 59572
Unclassified

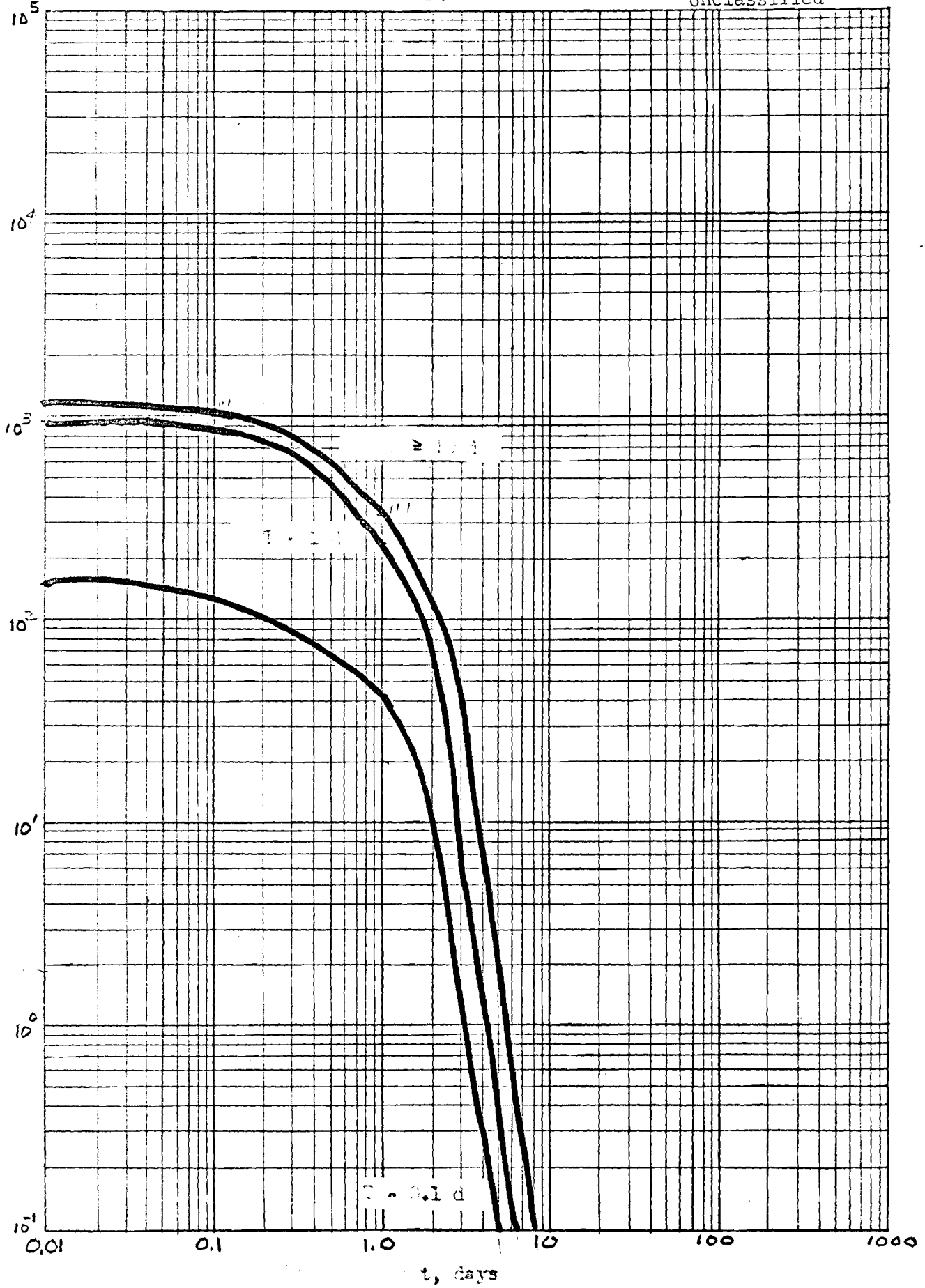

FIGURE 17 ACTIVATION DATA DOSE RATE AT THE SURFACE OF A SLAB AS A FUNCTION OF IRRADIATION TIME, T, AND DECAY TIME, t.

MATERIAL: LEAD GLASS PENBERTHY

ORNL-LR-Dwg. 59573
Unclassified

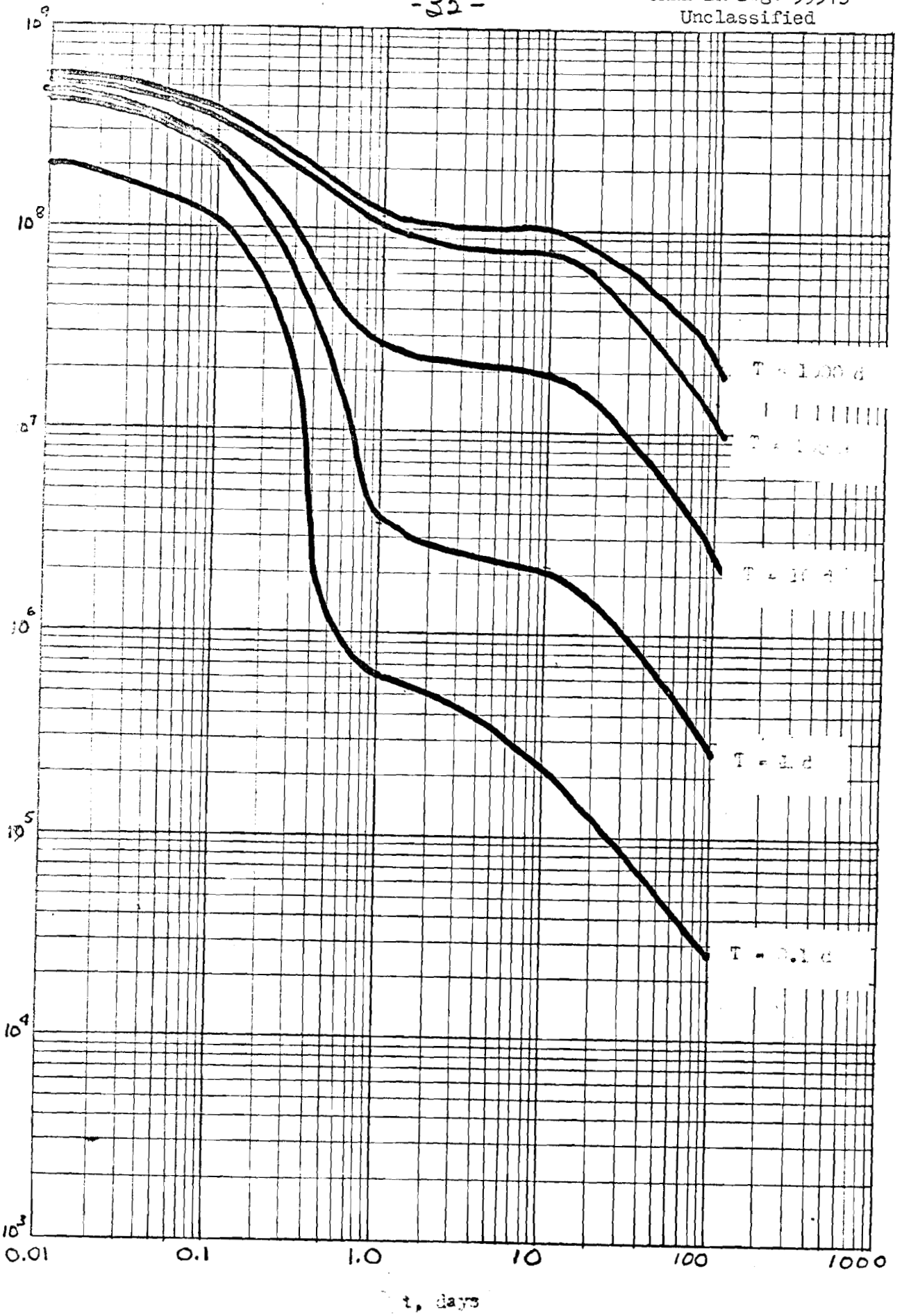

FIG. 18 ACTIVATION GAMMA ACTIVITY AS A FUNCTION OF IRRADIATION TIME, T, AND DECAY TIME, t.

ORNL-LR-Dwg. 59574
Unclassified

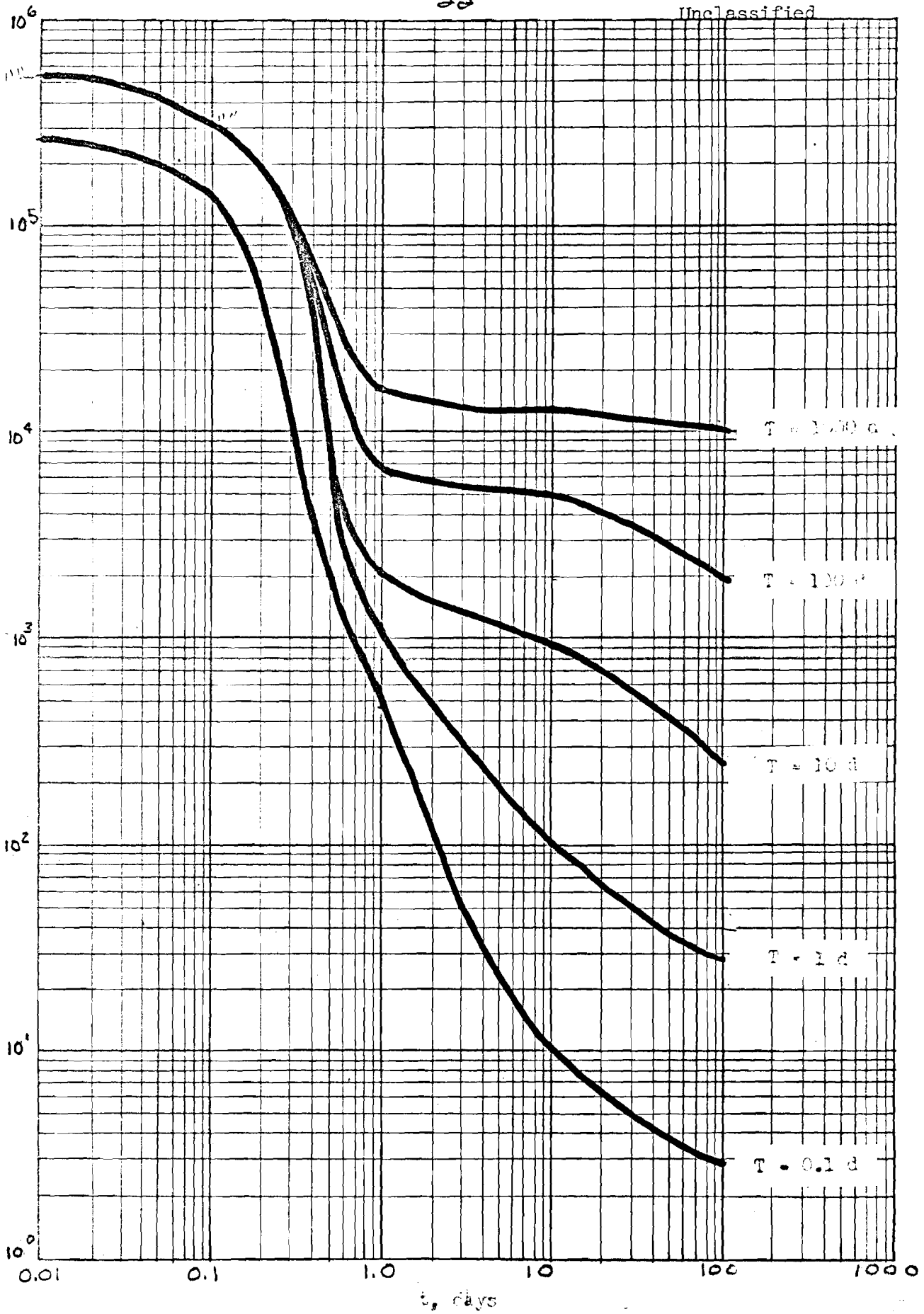

FIGURE 19 ACTIVATION GAMMA DOSE RATE AT THE SURFACE OF A SLAB AS A FUNCTION OF IRRADIATION TIME, T, AND DECAY TIME, t.

MATERIAL: 304L S.S.

ORNL-LR-Dwg. 59575
Unclassified

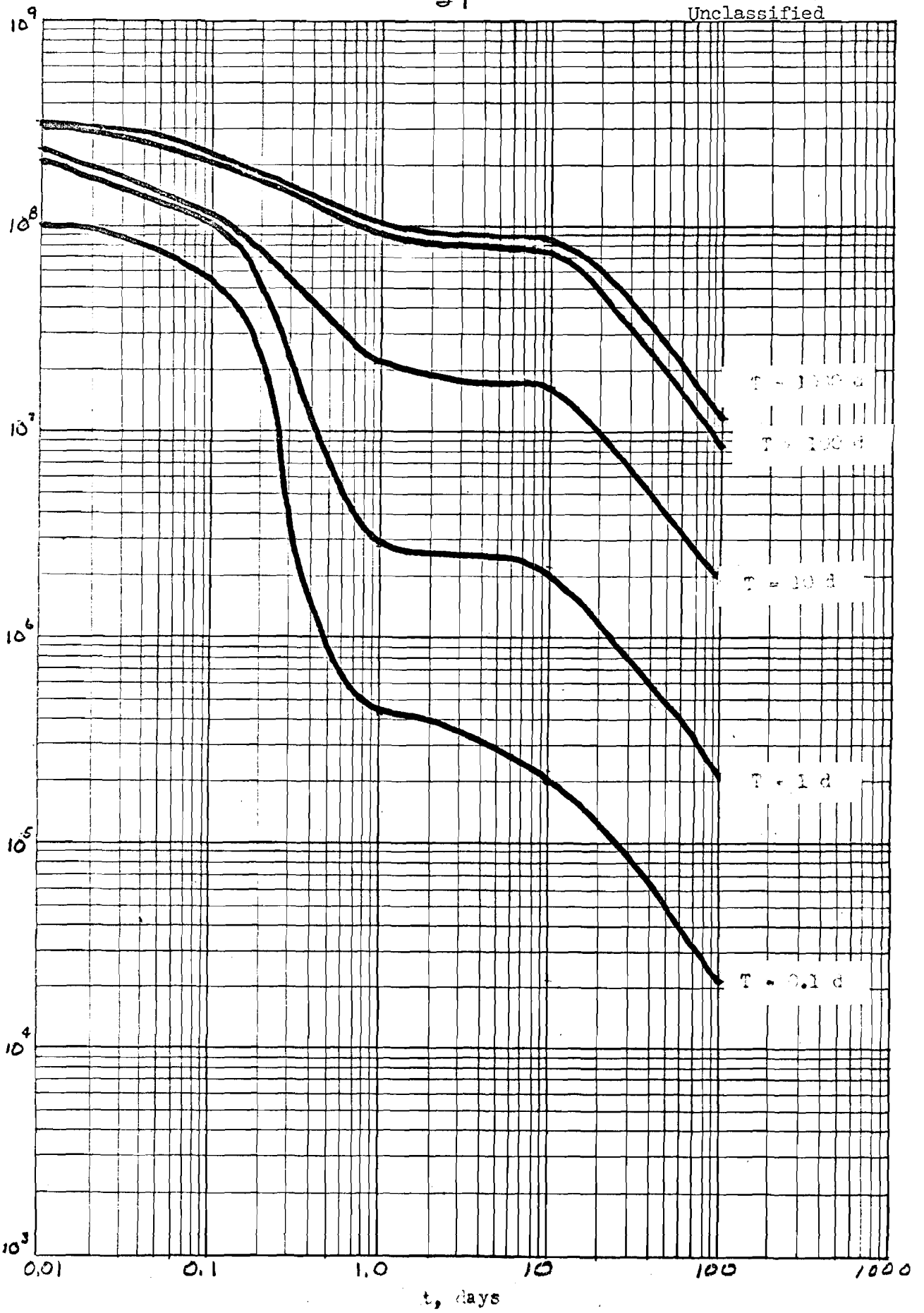

20 ACTIVATION GAMMA ACTIVITY AS A FUNCTION OF IRRADIATION TIME, T, AND DECAY TIME, t.

ORNL-LR-Dwg. 59576
Unclassified

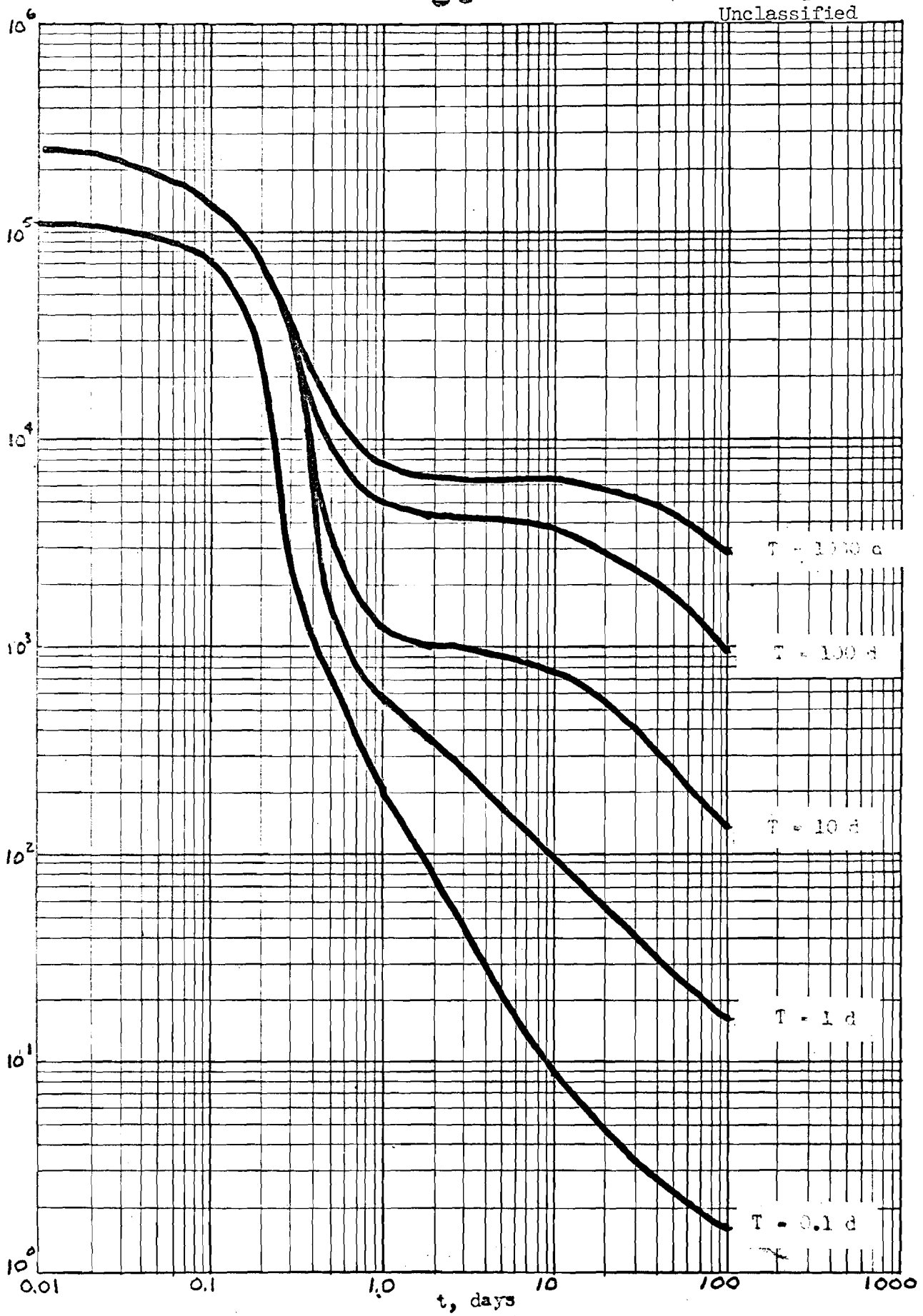

FIGURE 21 ACTIVATION GAMMA DOSE RATE AT THE SURFACE OF A SLAB AS A FUNCTION OF IRRADIATION TIME, T, AND DECAY TIME, t.

MATERIAL: 440A S.S

ORNL-LR-Dwg. 59577
Unclassified

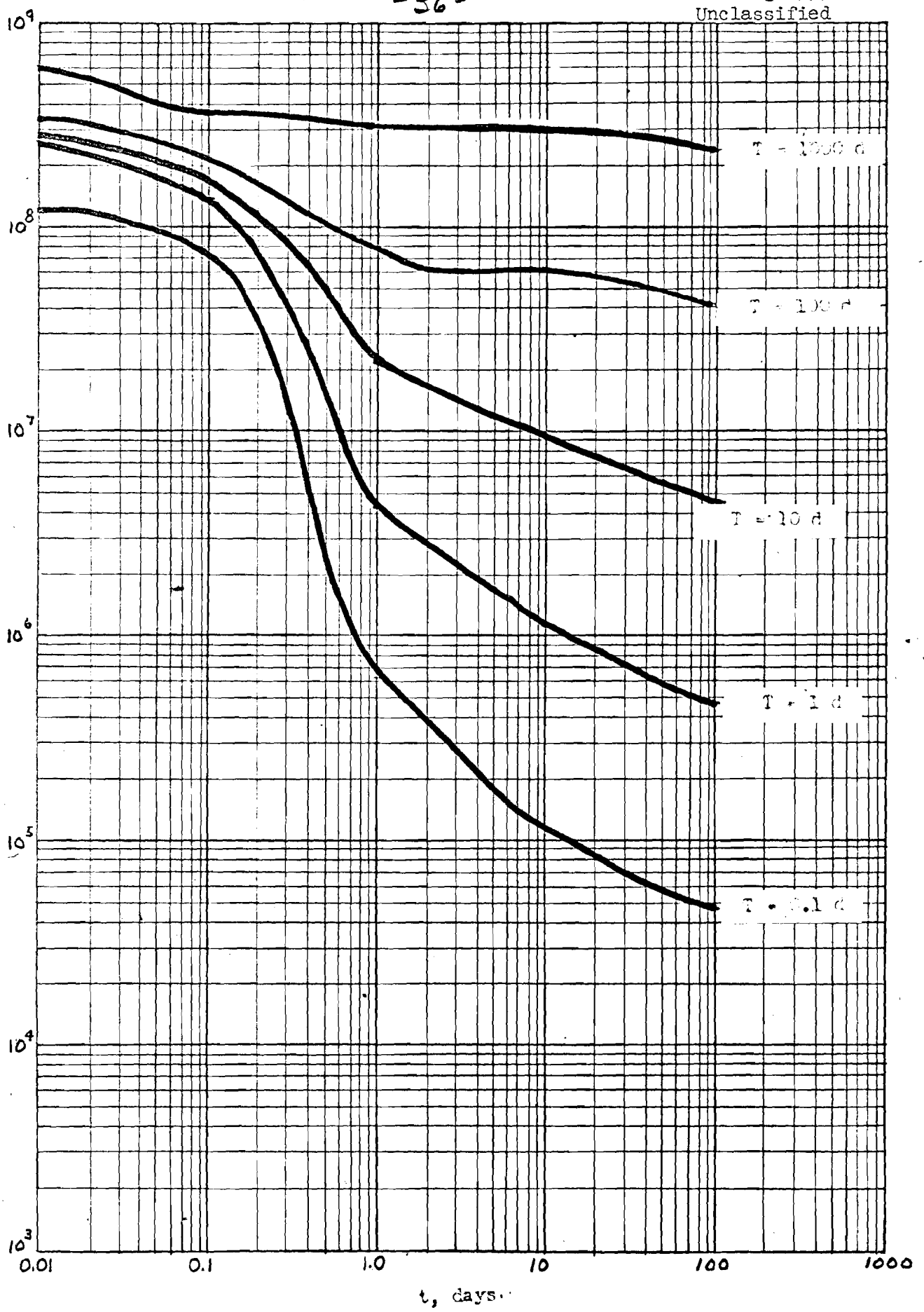

FIGURE 22 ACTIVATION GAMMA ACTIVITY AS A FUNCTION OF IRRADIATION TIME, T, AND DECAY TIME, t.

ORNL-LR-Dwg. 59578
Unclassified

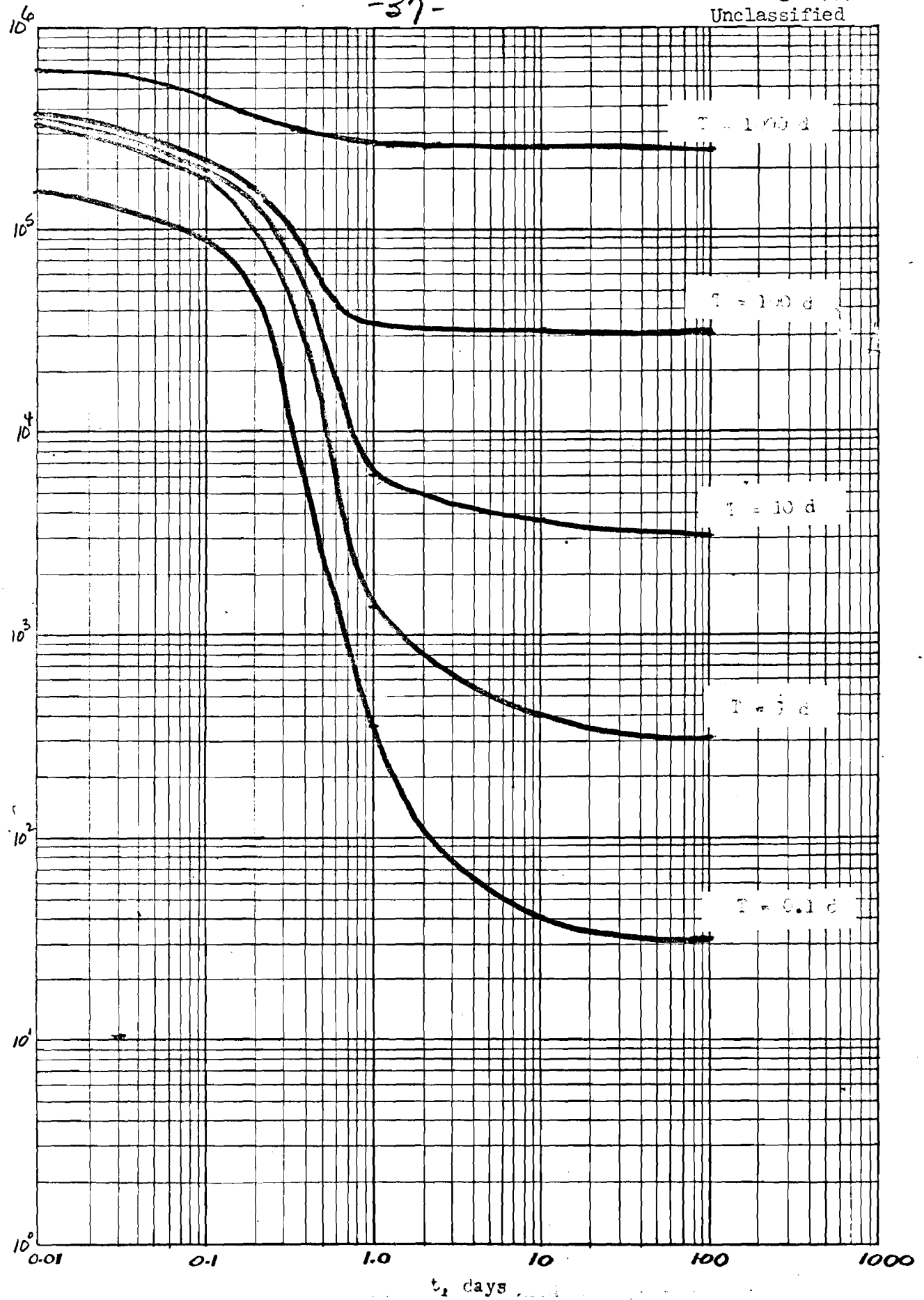

FIG. 23 GAMMA DOSE RATE AT THE SURFACE OF A SLAB AS A FUNCTION OF IRRADIATION TIME, T, AND DECAY TIME, t.

MATERIAL: HASTELLOY B

ORNL-LR-Dwg. 59579
Unclassified

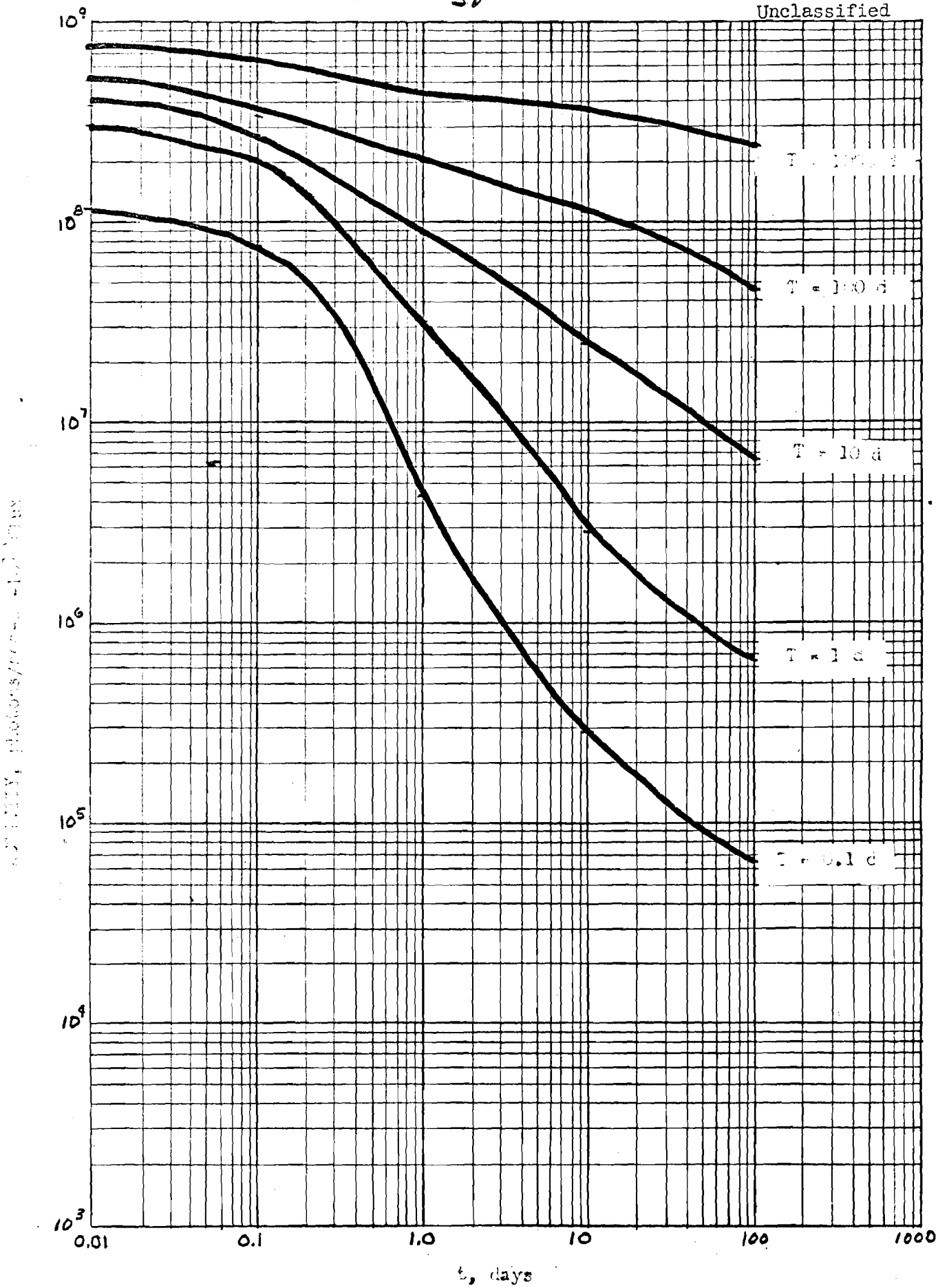

FIGURE 24 ACTIVATION GAMMA ACTIVITY AS A FUNCTION OF IRRADIATION TIME, T, AND DECAY TIME, t

ORNL-LR-Dwg. 59580
Unclassified

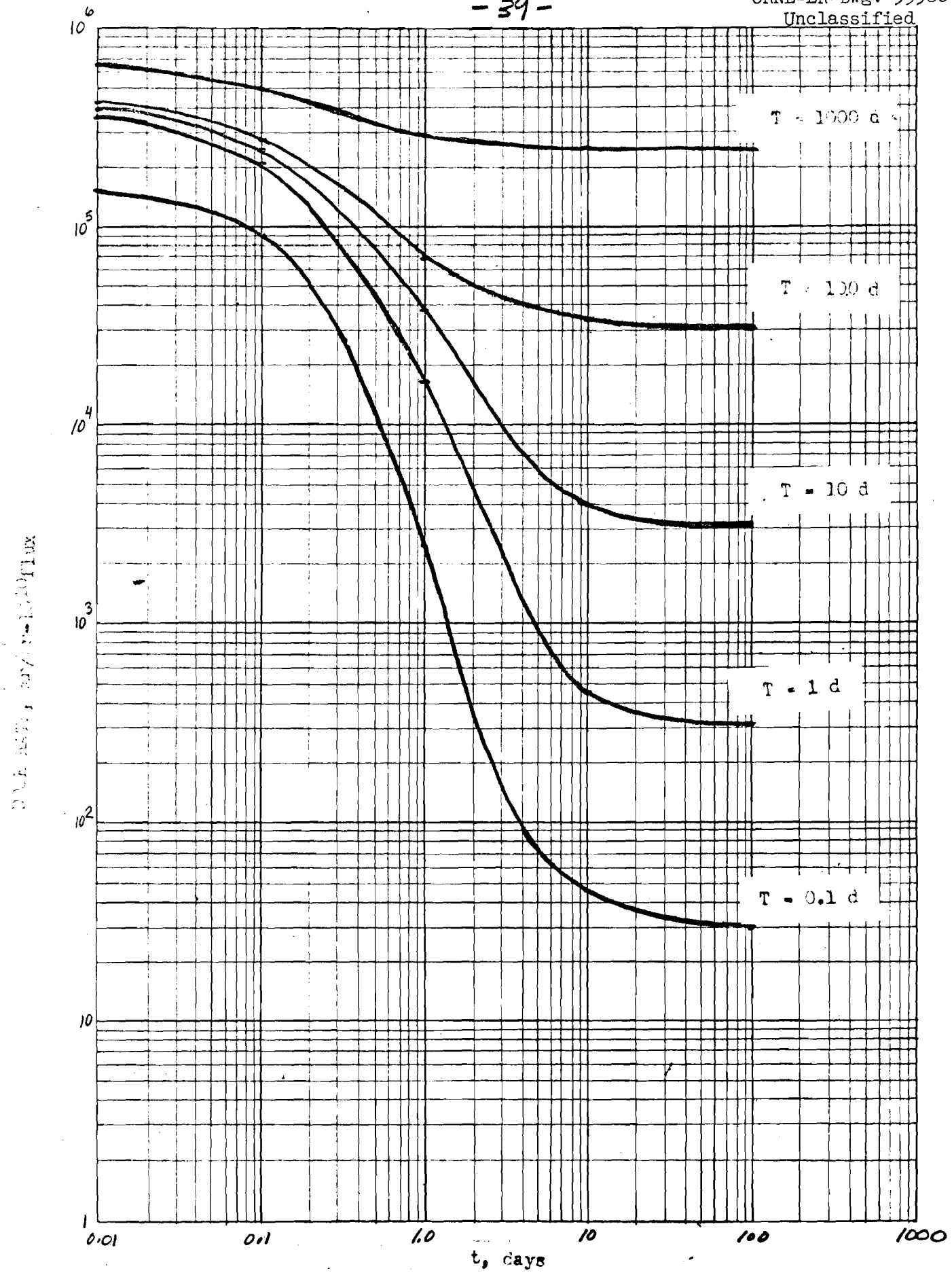

FIGURE 25 ACTIVATION GAMMA DOSE RATE AT THE SURFACE OF A SLAB AS A FUNCTION OF IRRADIATION TIME, T, AND DECAY TIME, t.

MATERIAL: HASTELLOY C

ORNL-LR-Dwg. 59581
Unclassified

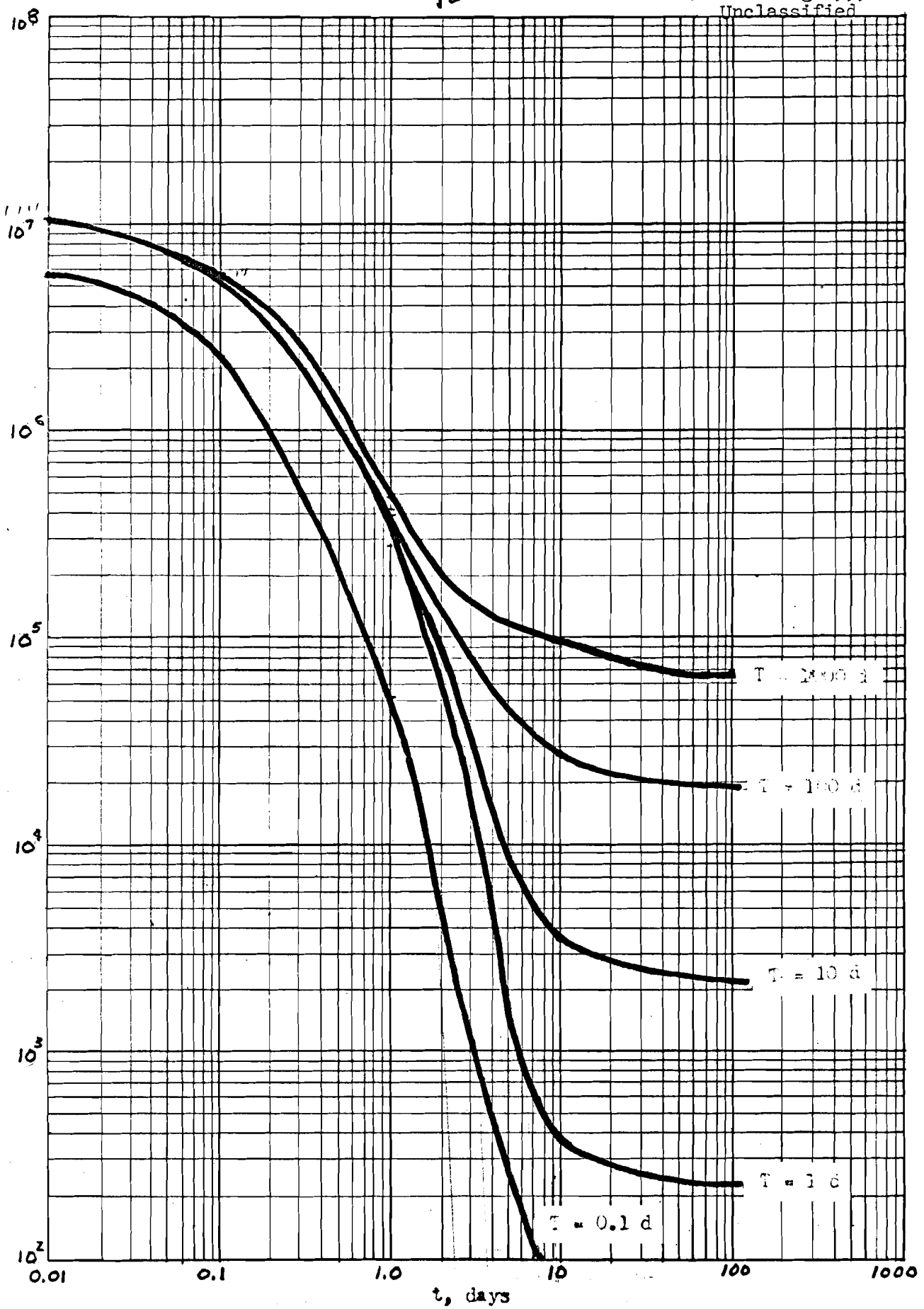

FIGURE 26 ACTIVATION GAMMA ACTIVITY AS A FUNCTION OF IRRADIATION TIME, T, AND DECAY TIME, t.

ORNL-LR-Dwg. 59582
Unclassified

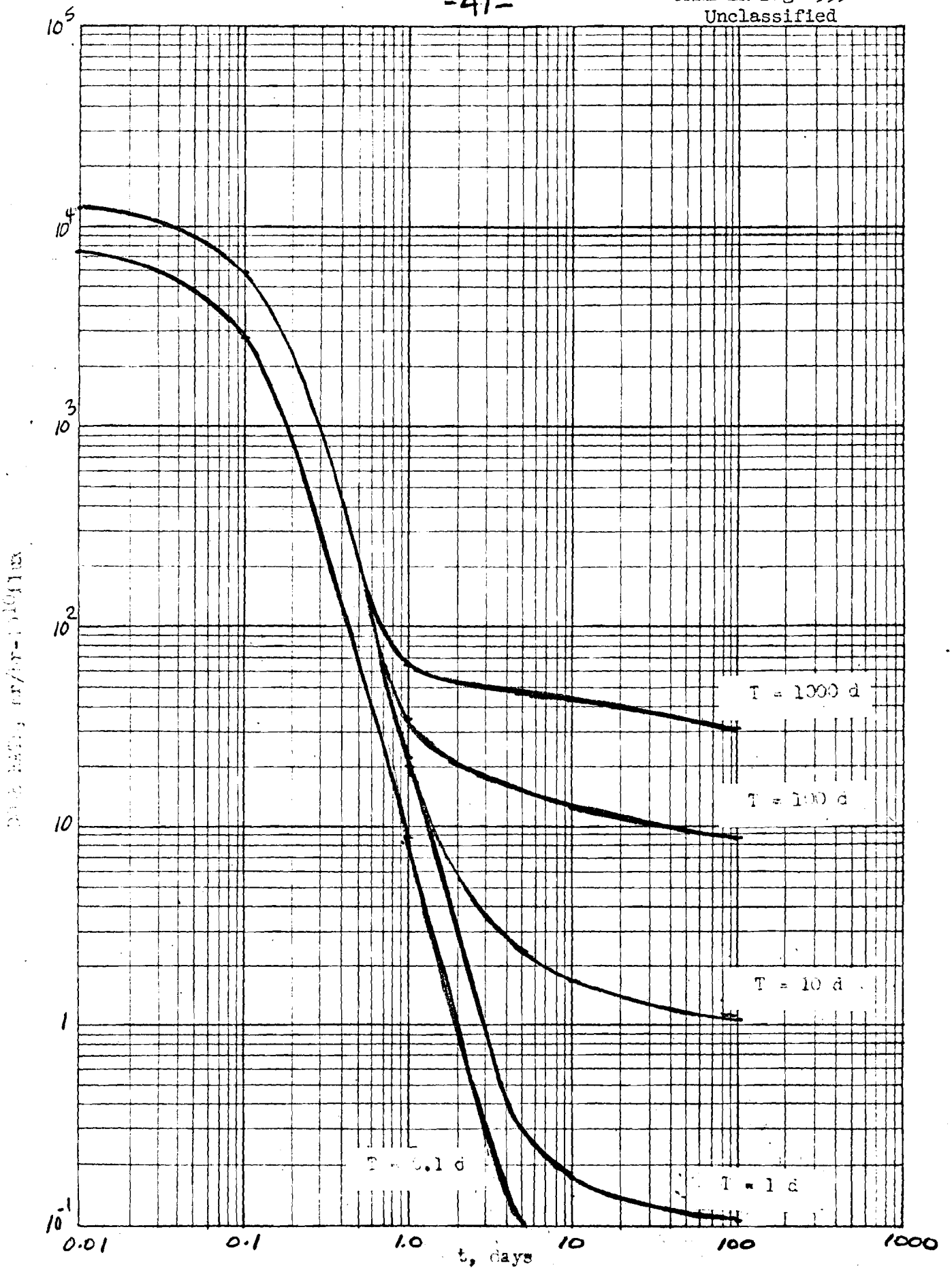

FIGURE 27 ACTIVATION GAMMA DOSE RATE AT THE SURFACE OF A SLAB AS A FUNCTION OF IRRADIATION TIME, T, AND DECAY TIME, t.

ORNL-LR-Dwg. 59583
Unclassified

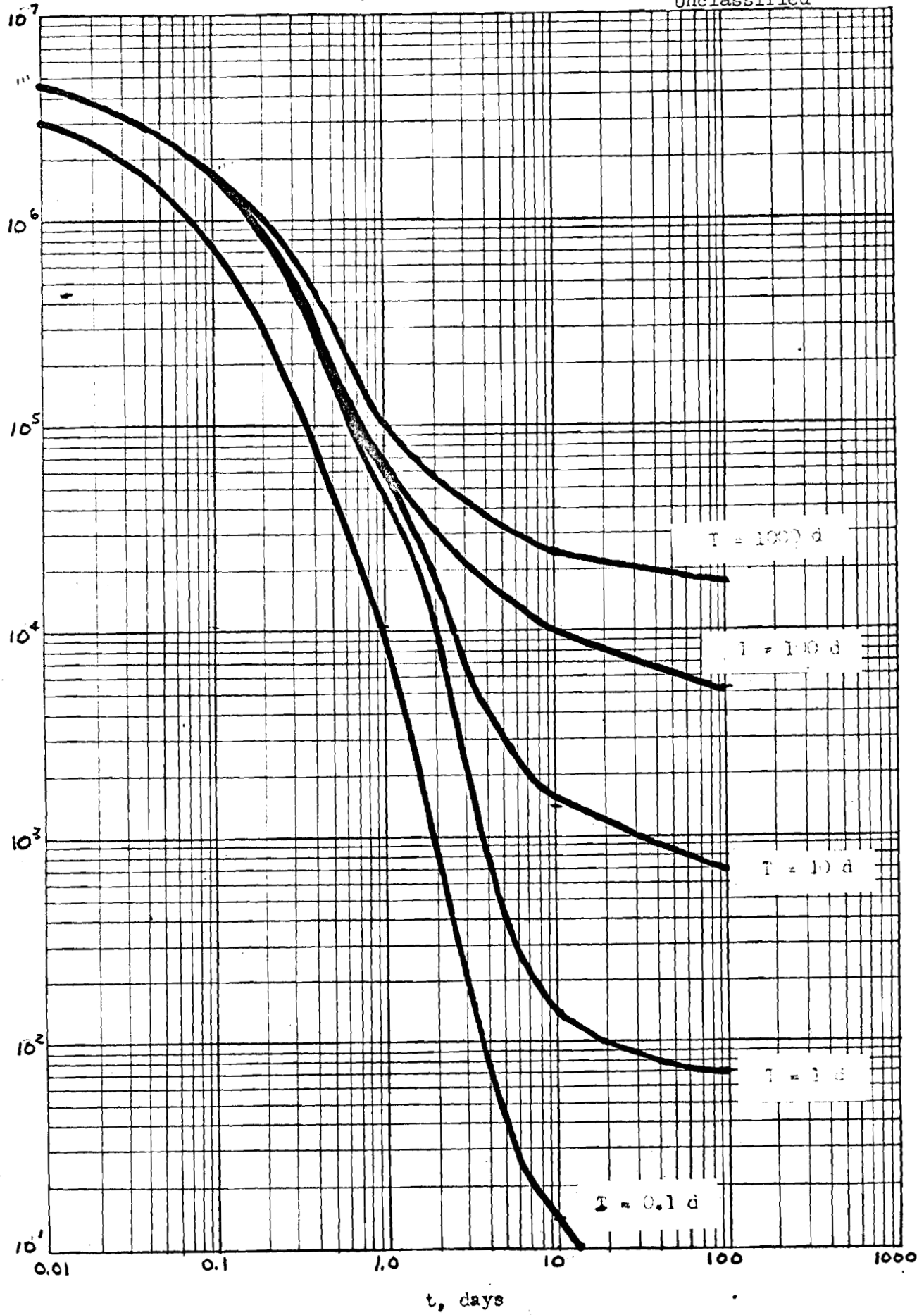

FIGURE 28 ACTIVATION GAMMA ACTIVITY AS A FUNCTION OF IRRADIATION TIME, T, AND DECAY TIME, t.

ORNL-LR-Dwg. 59584
Unclassified

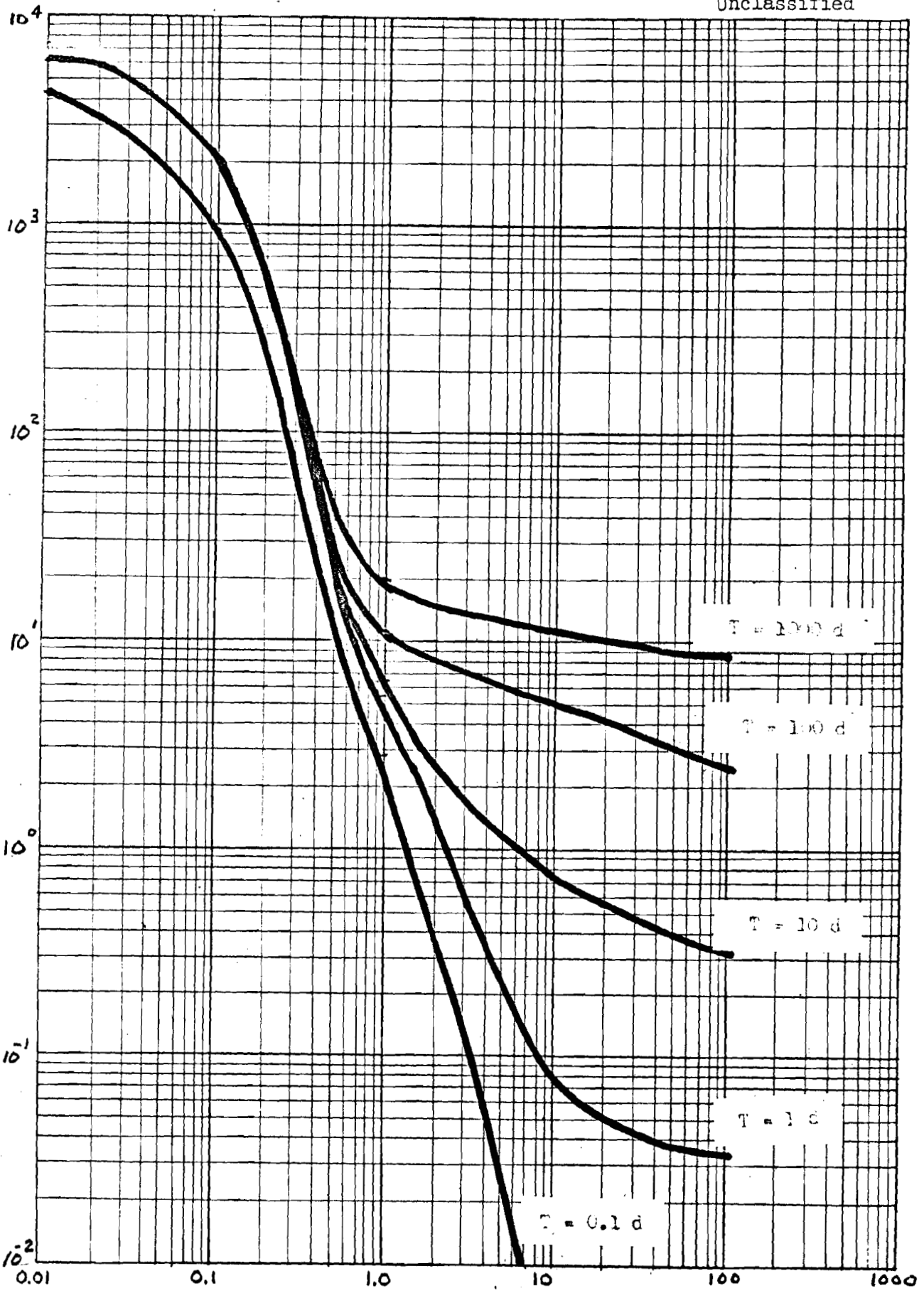

FIGURE 29 ACTIVATION GAMMA DOSE RATE AT THE SURFACE OF A SLAB AS A FUNCTION OF IRRADIATION TIME, T, AND DECAY TIME, t.

MATERIAL: ALUMINUM 1050

ORNL-LR-Dwg. 59585
Unclassified

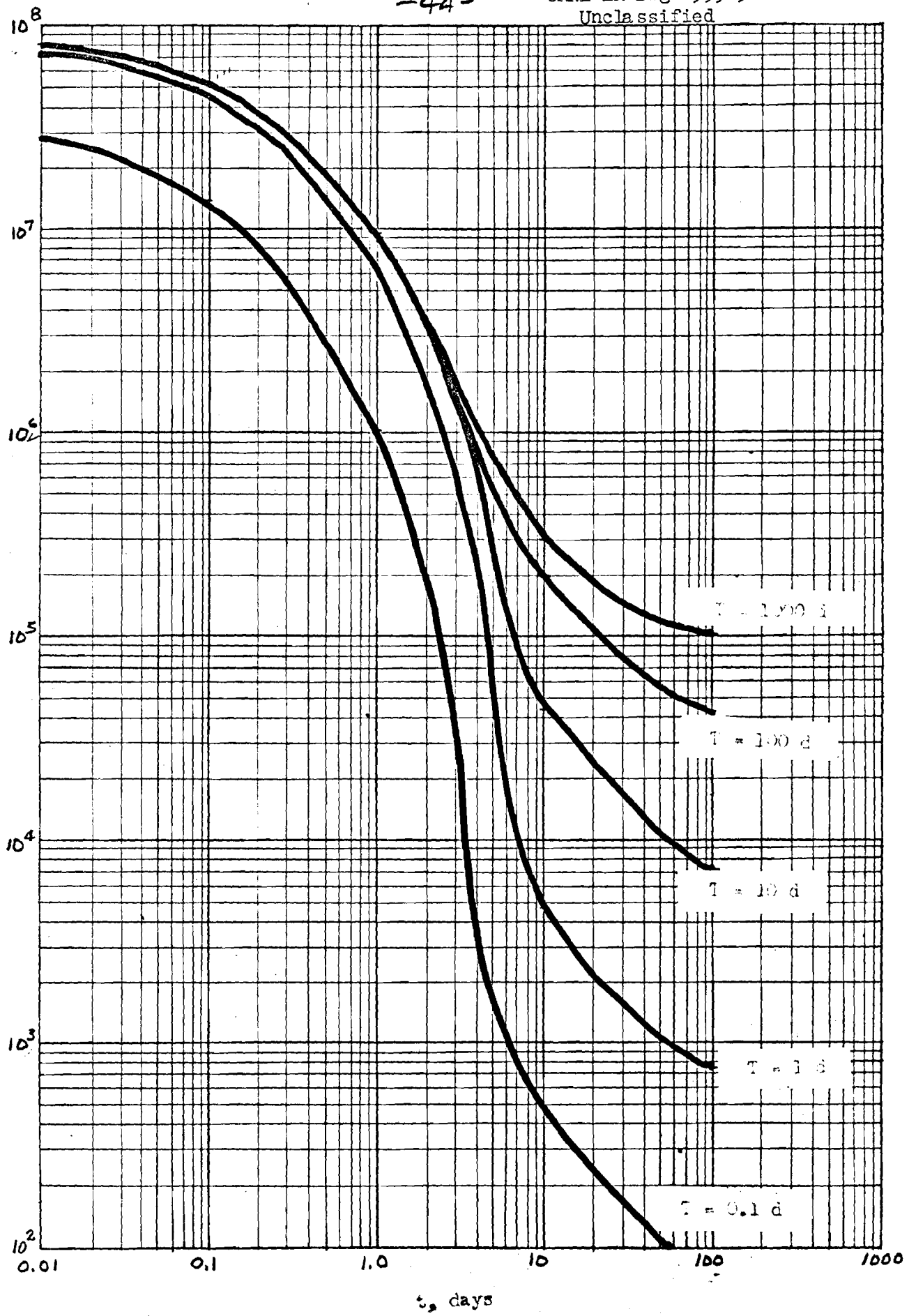

FIGURE 30 ACTIVATION GAMMA ACTIVITY AS A FUNCTION OF IRRADIATION TIME, T, AND DECAY TIME, t.

ORNL-LR-Dwg. 59586
Unclassified

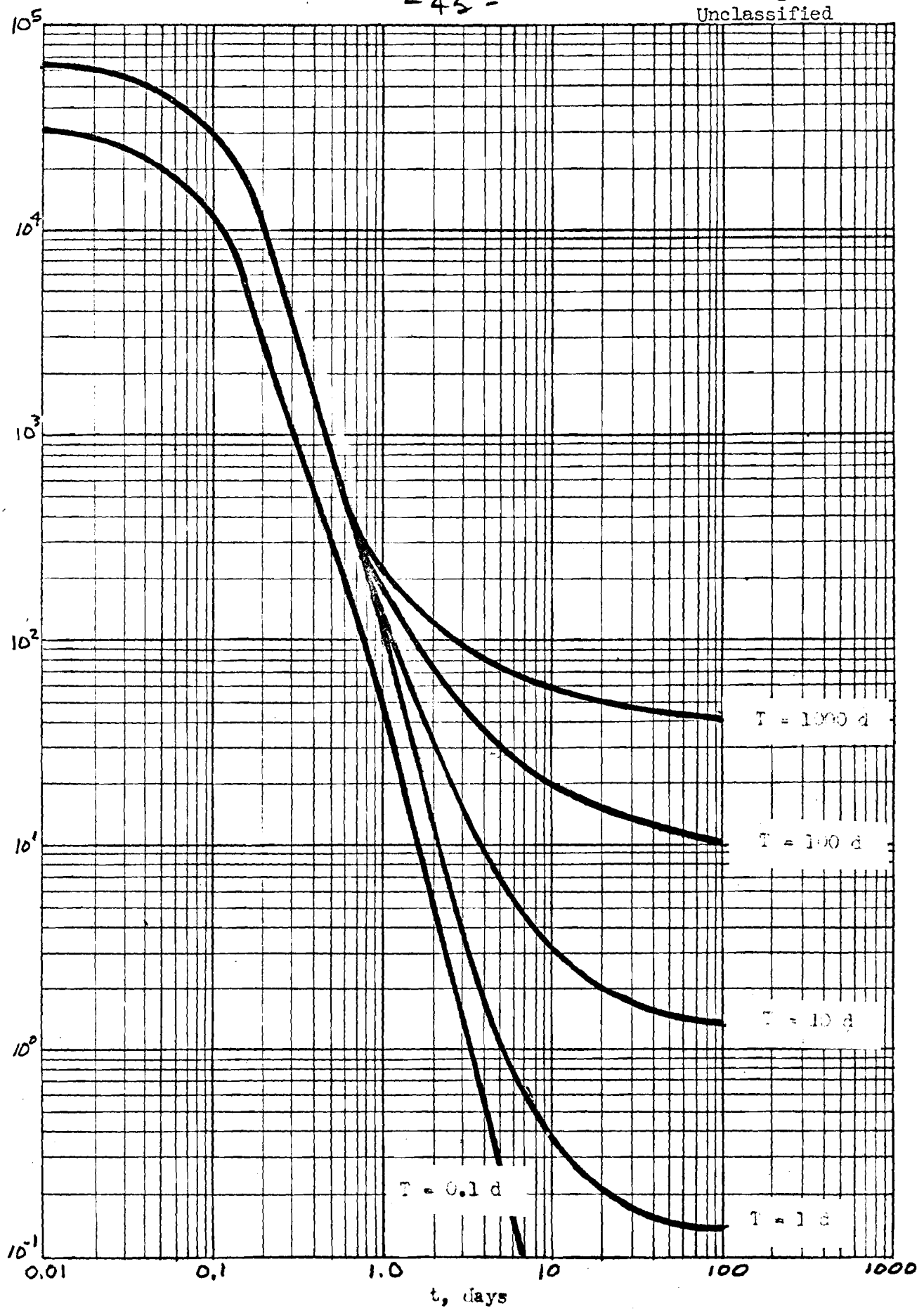

FIGURE 31 ACTIVATION GAMMA DOSE RATE AT THE SURFACE OF A SLAB AS A FUNCTION OF IRRADIATION TIME, T, AND DECAY TIME, t.

MATERIAL: ALUMINUM 2024

ORNL-LR-Dwg. 59587
Unclassified

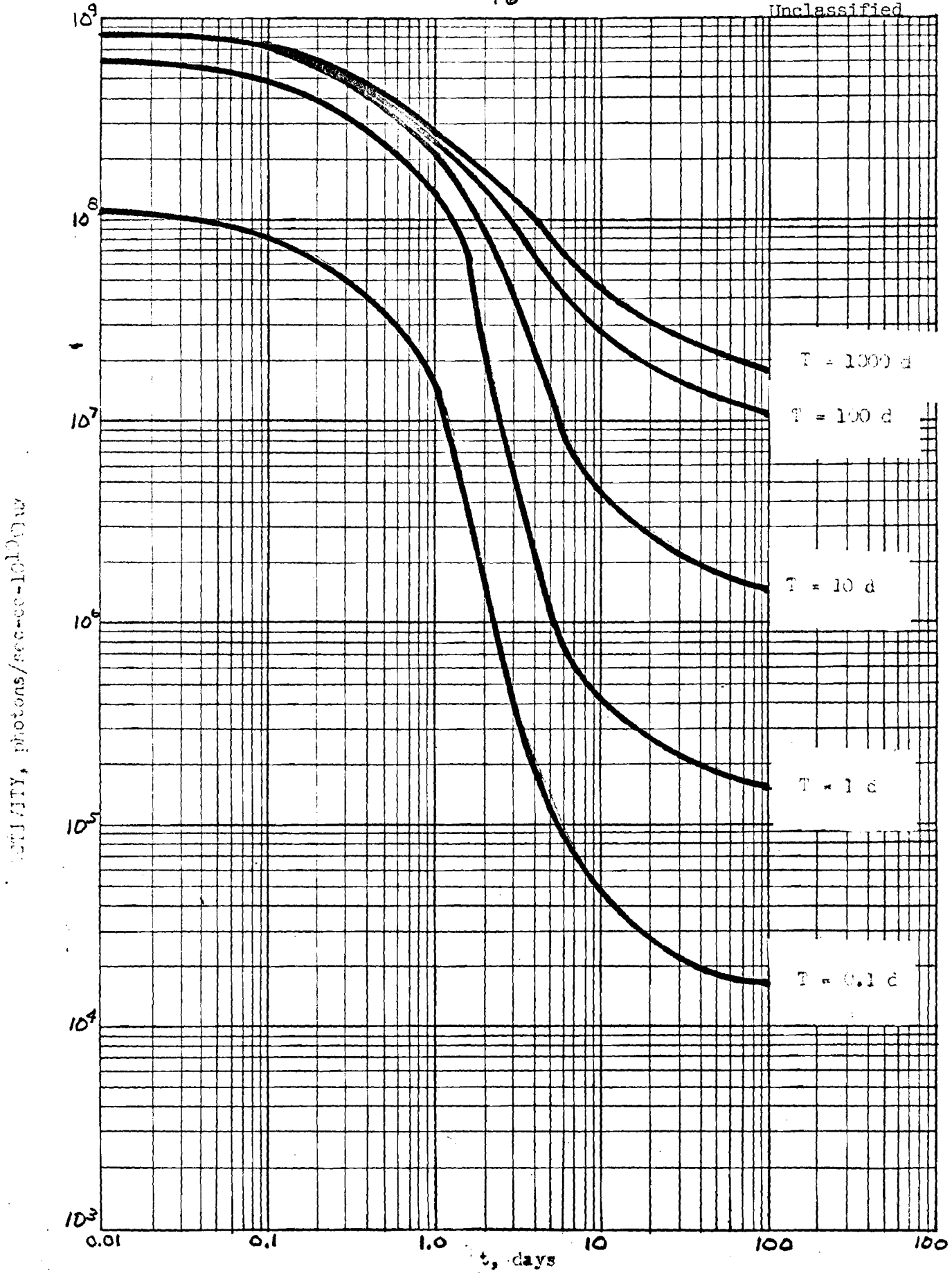

FIGURE 32 ACTIVATION GAMMA ACTIVITY AS A FUNCTION OF IRRADIATION TIME, T, AND DECAY TIME, t.

ORNL-LR-Dwg. 59588
Unclassified

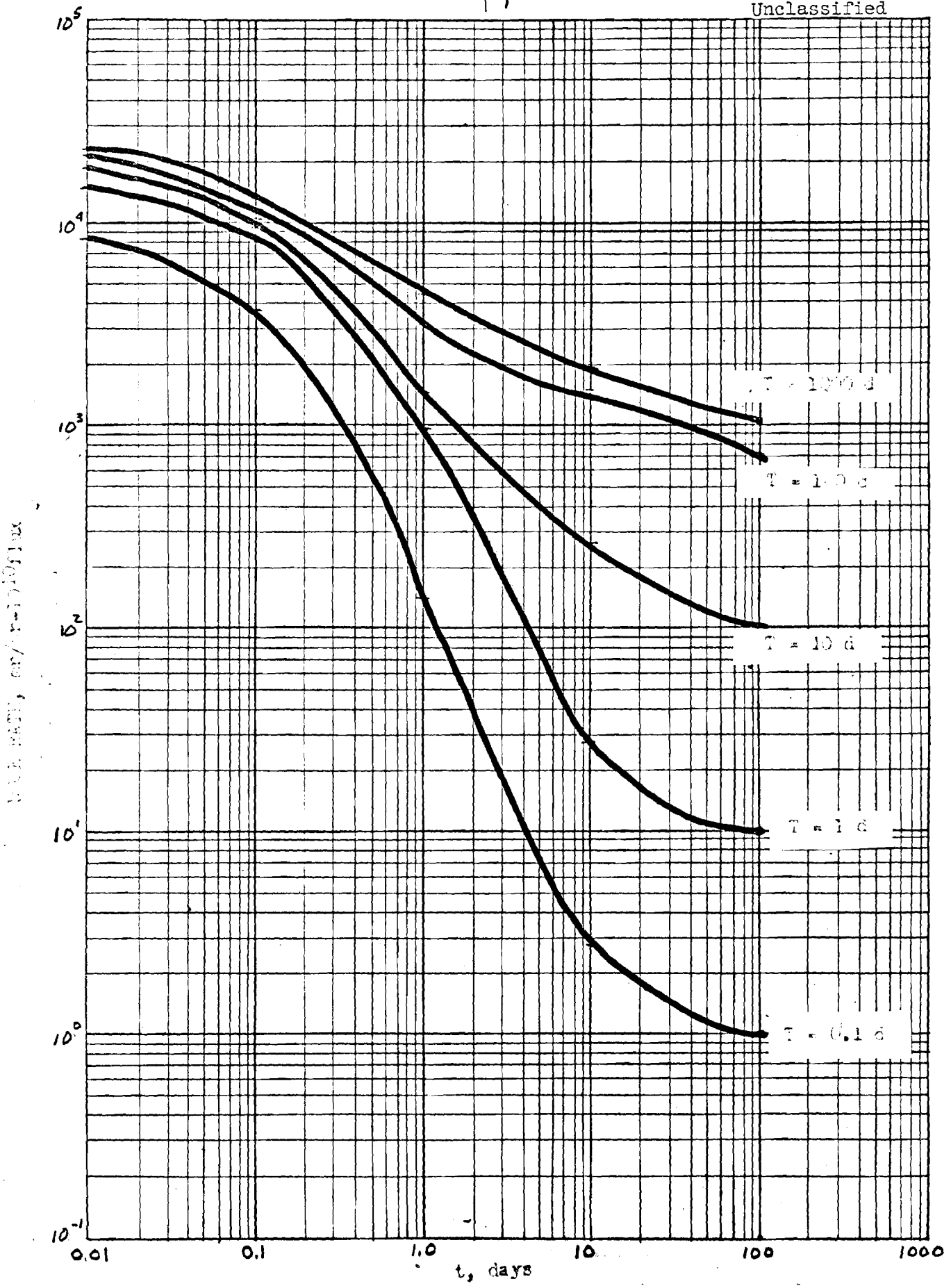

FIGURE 33 ACTIVATION GAMMA DOSE RATE AT THE SURFACE OF A SLAB AS A FUNCTION OF IRRADIATION TIME, T, AND DECAY TIME, t.

MATERIAL: Magnesium

ORNL-LR-Dwg. 59589
Unclassified

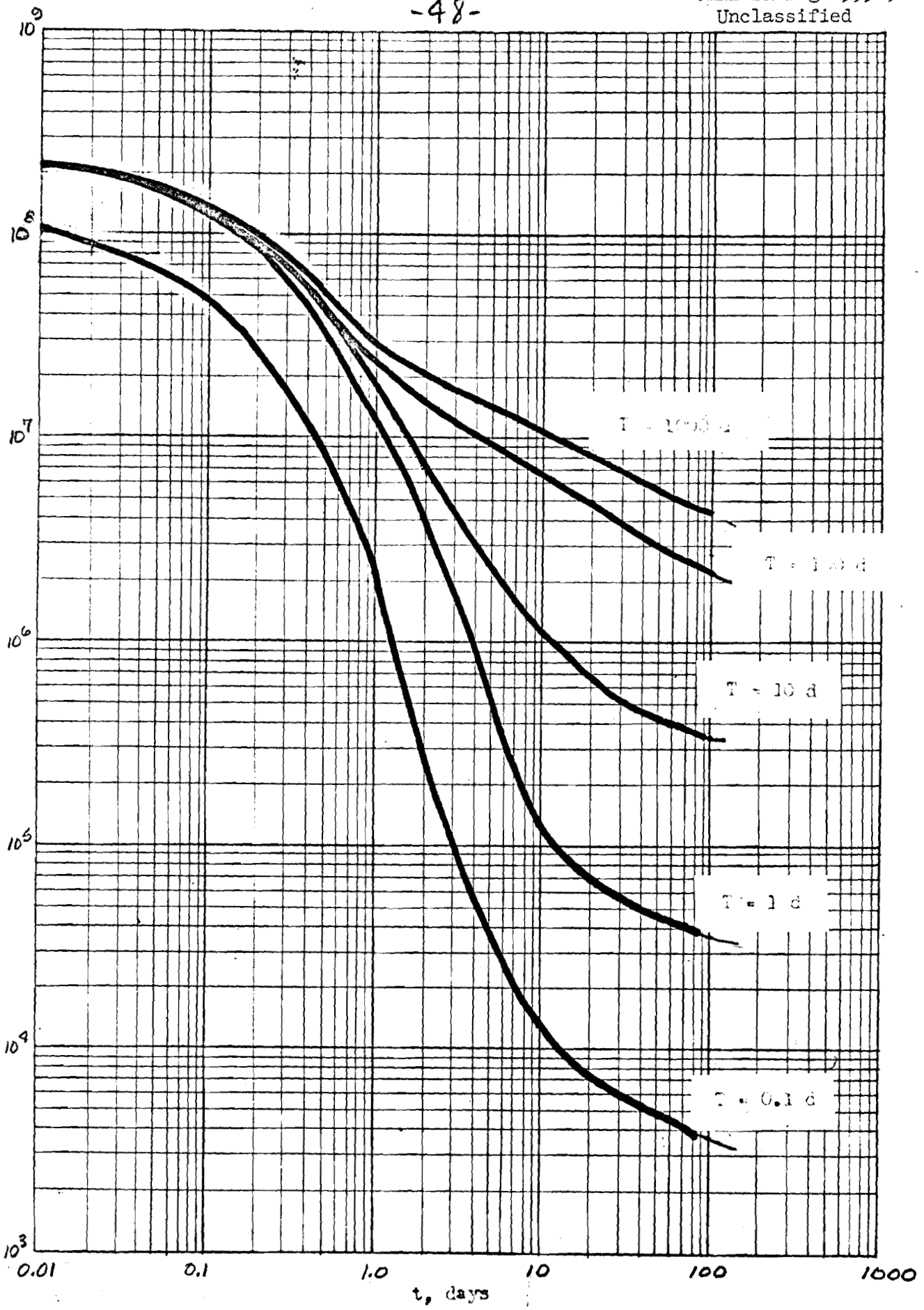

FIGURE 34 ACTIVATION GAMMA ACTIVITY AS A FUNCTION OF IRRADIATION TIME, T, AND DECAY TIME, t.

ORNL-LR-Dwg. 59590
Unclassified

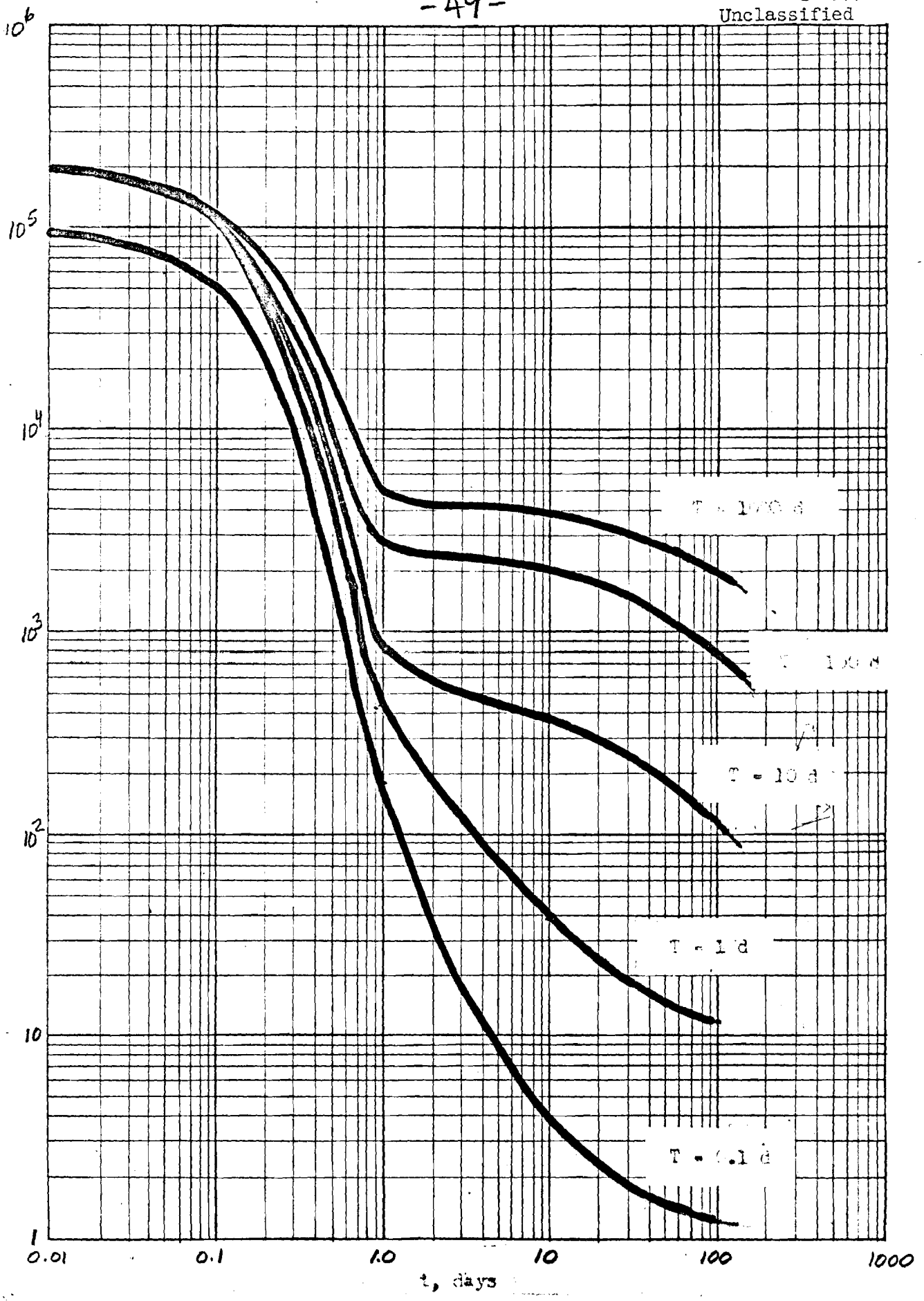

FIG. 35 [illegible] DISSIPATION DATA DOSE RATE AT THE SURFACE OF A SLAB AS A FUNCTION OF IRRADIATION TIME, T, AND DECAY TIME, t.

[illegible] CARBON STEEL

ORNL-LR-Dwg. 59591
Unclassified

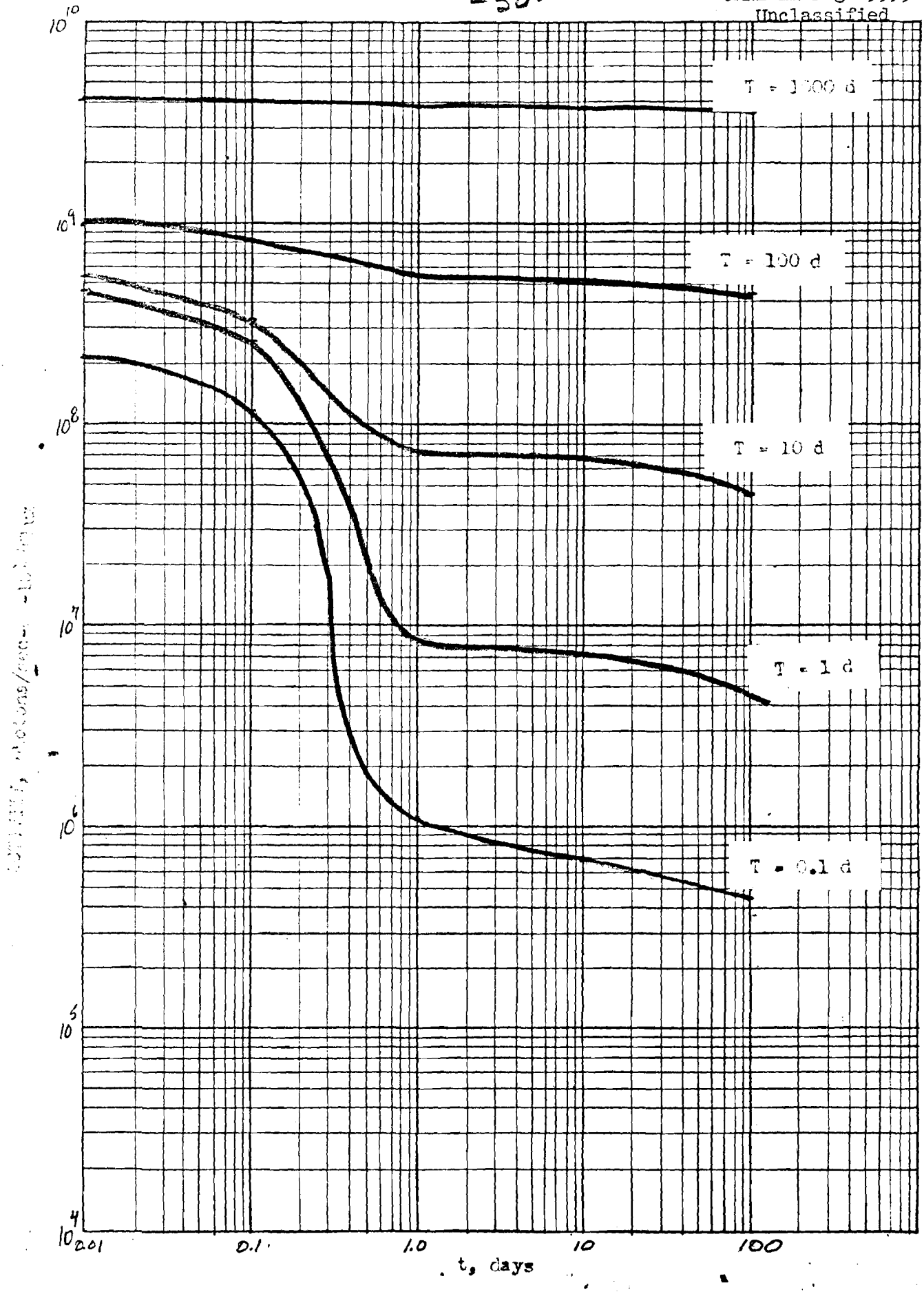

FIGURE 36 ACTIVATION GAMMA ACTIVITY AS A FUNCTION OF IRRADIATION TIME, T, AND DECAY TIME, t.

ORNL-LR-Dwg. 59592
Unclassified

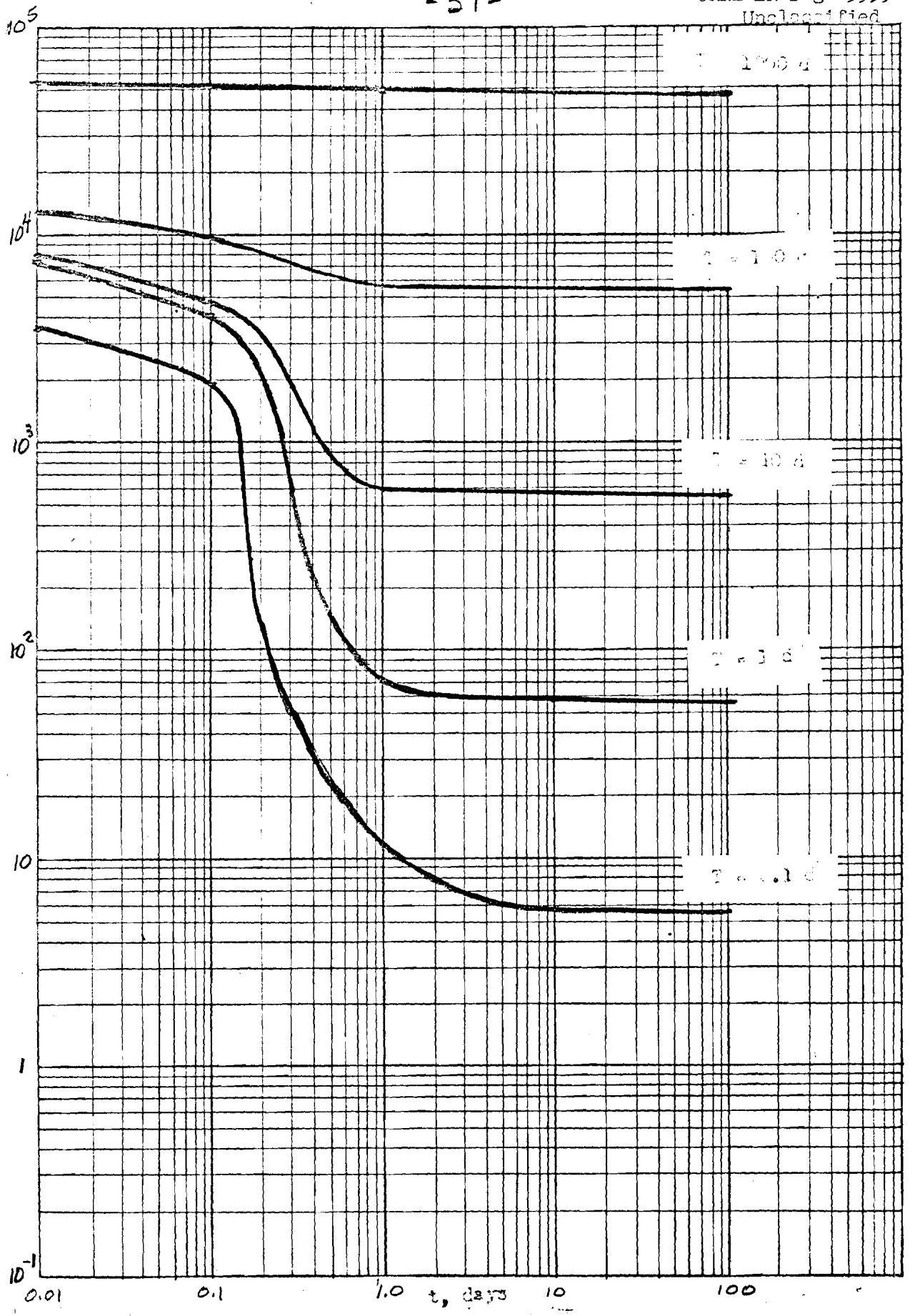

FIGURE 37 ACTIVATION DATA DUE TO BARE AT THE SURFACE OF A SLAB AS A FUNCTION OF IRRADIATION TIME, T, AND DECAY TIME, t.

MATERIAL: ELGILOY

ORNL-LR-Dwg. 59593
Unclassified

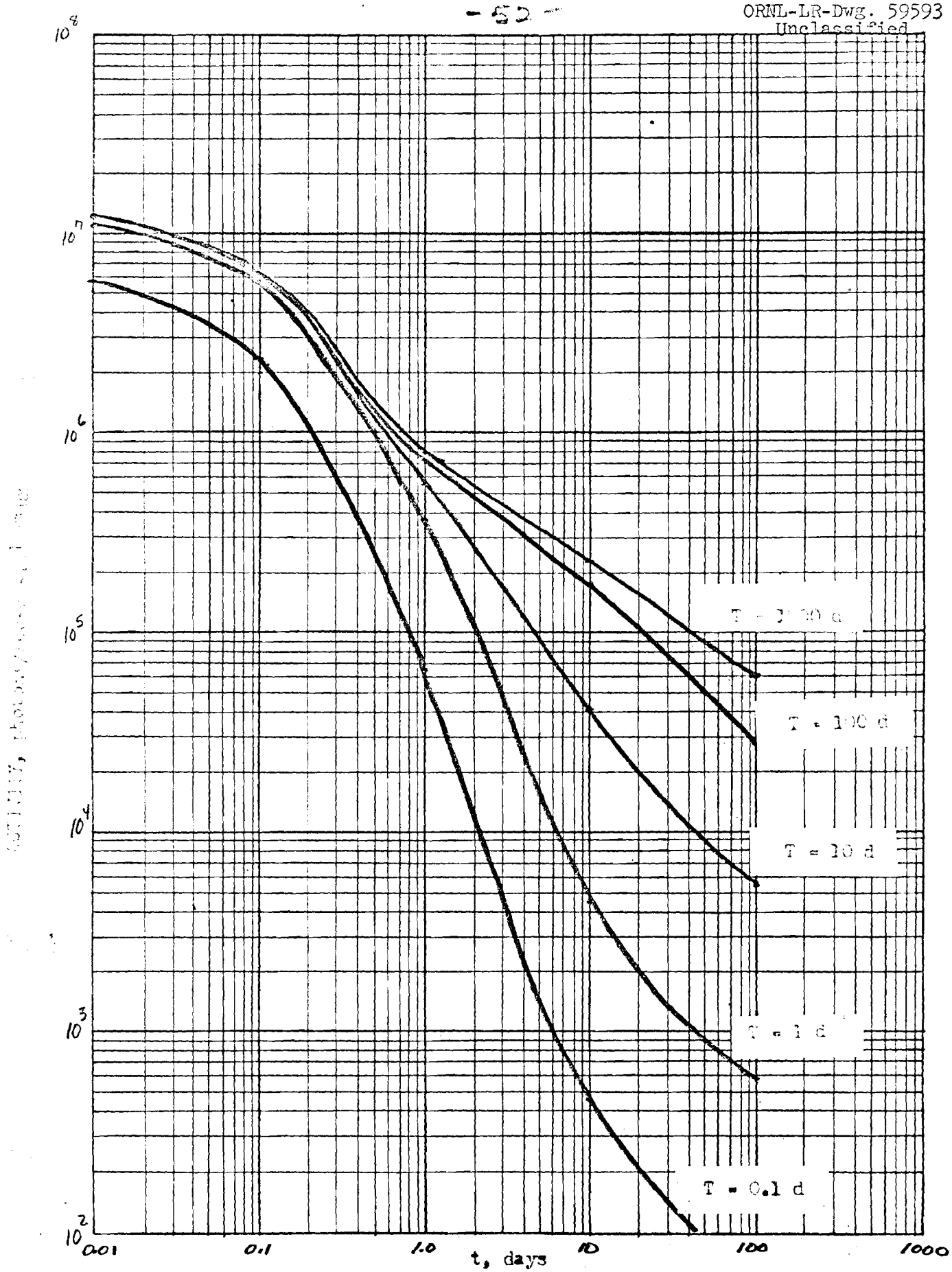

FIGURE 38 ACTIVATION GAMMA ACTIVITY AS A FUNCTION OF IRRADIATION TIME, T, AND DECAY TIME, t.

ORNL-LR-Dwg. 59594
Unclassified

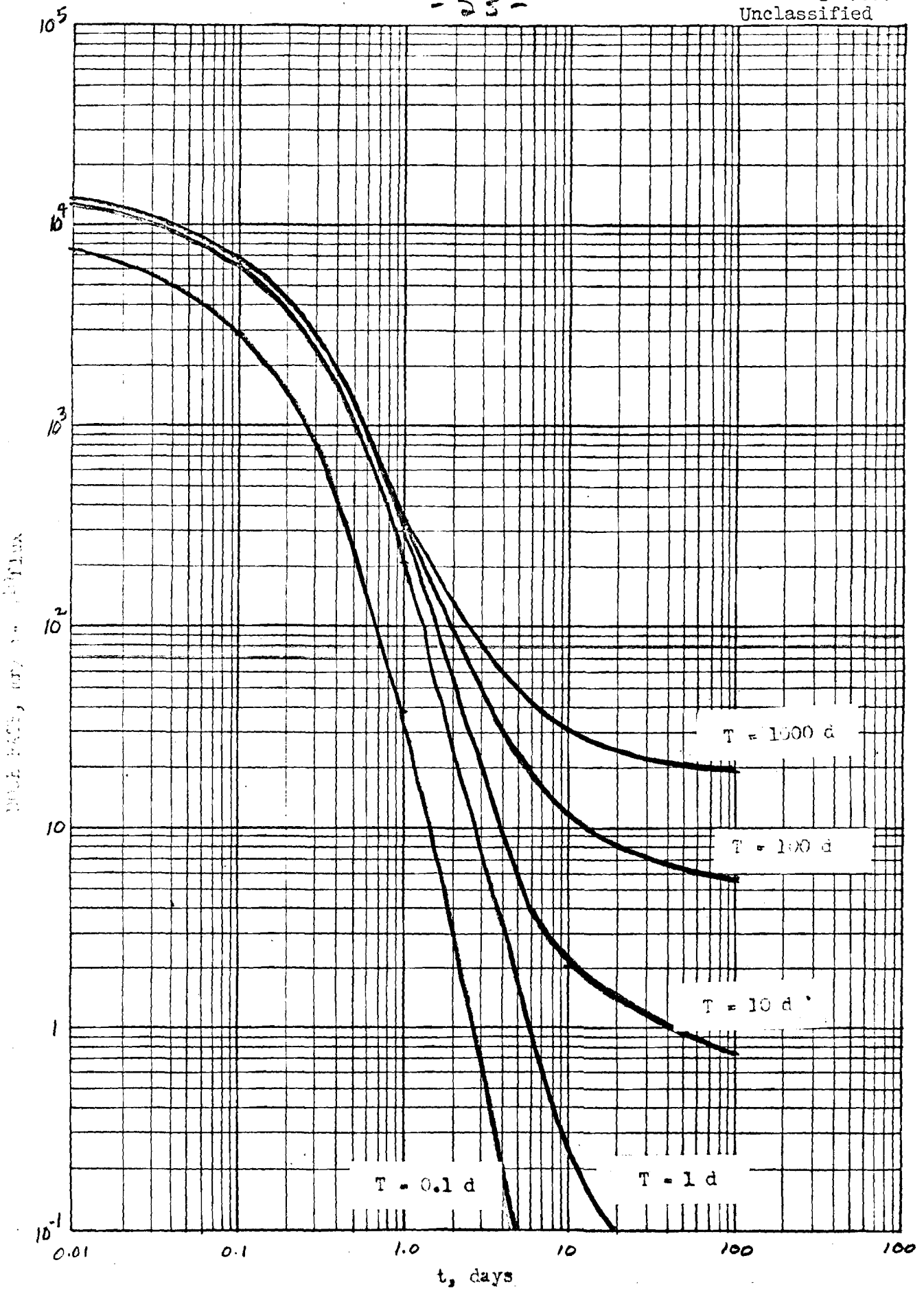

FIGURE 39 ACTIVATION GAMMA DOSE RATE AT THE SURFACE OF A SLAB AS A FUNCTION OF IRRADIATION TIME, T, AND DECAY TIME, t.

MATERIAL: Al-206.35

ORNL-LR-Dwg. 59595
Unclassified

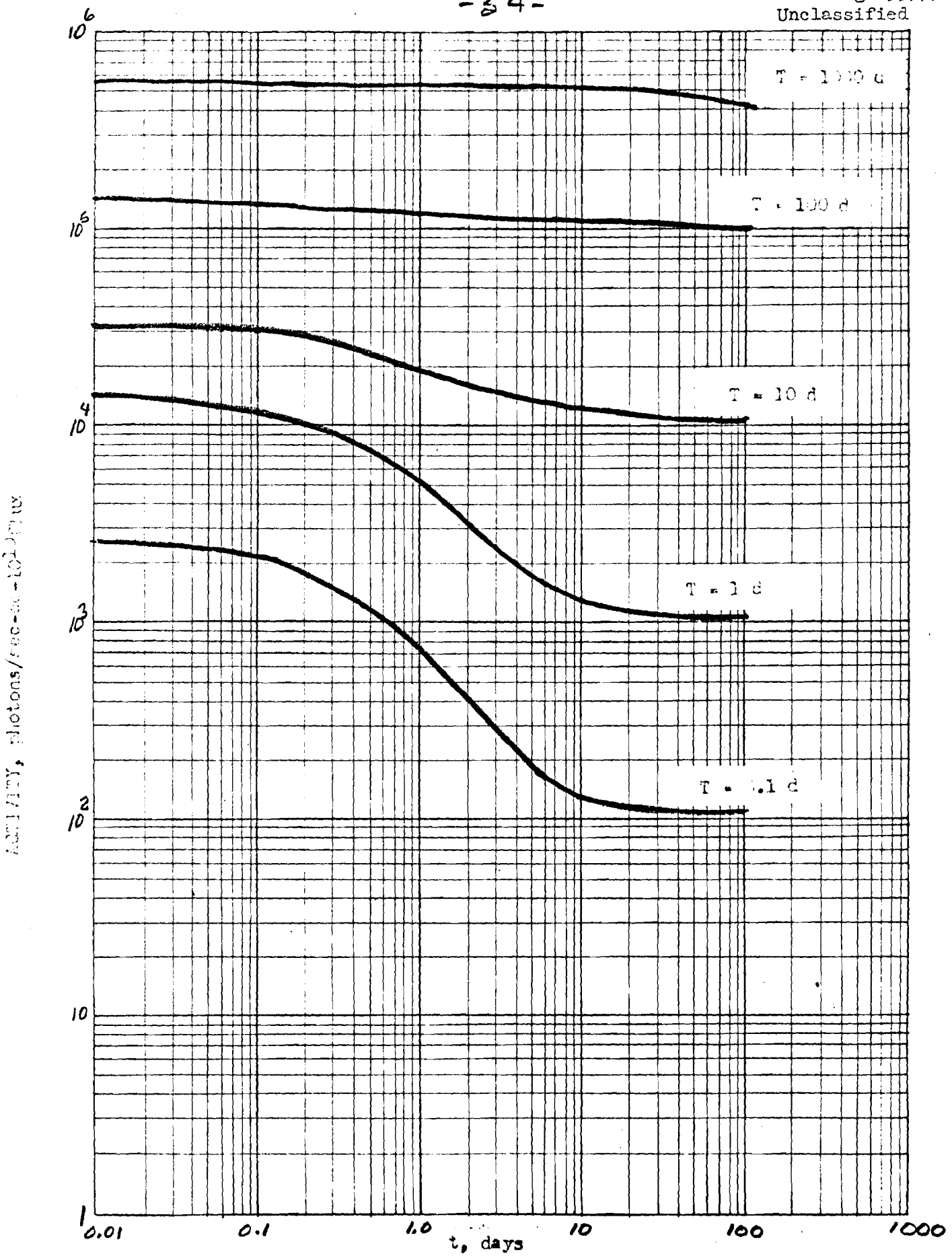

FIGURE 40 ACTIVATION GAMMA ACTIVITY AS A FUNCTION OF IRRADIATION TIME, T, AND DECAY TIME, t.

ORNL-LR-Dwg. 59596
Unclassified

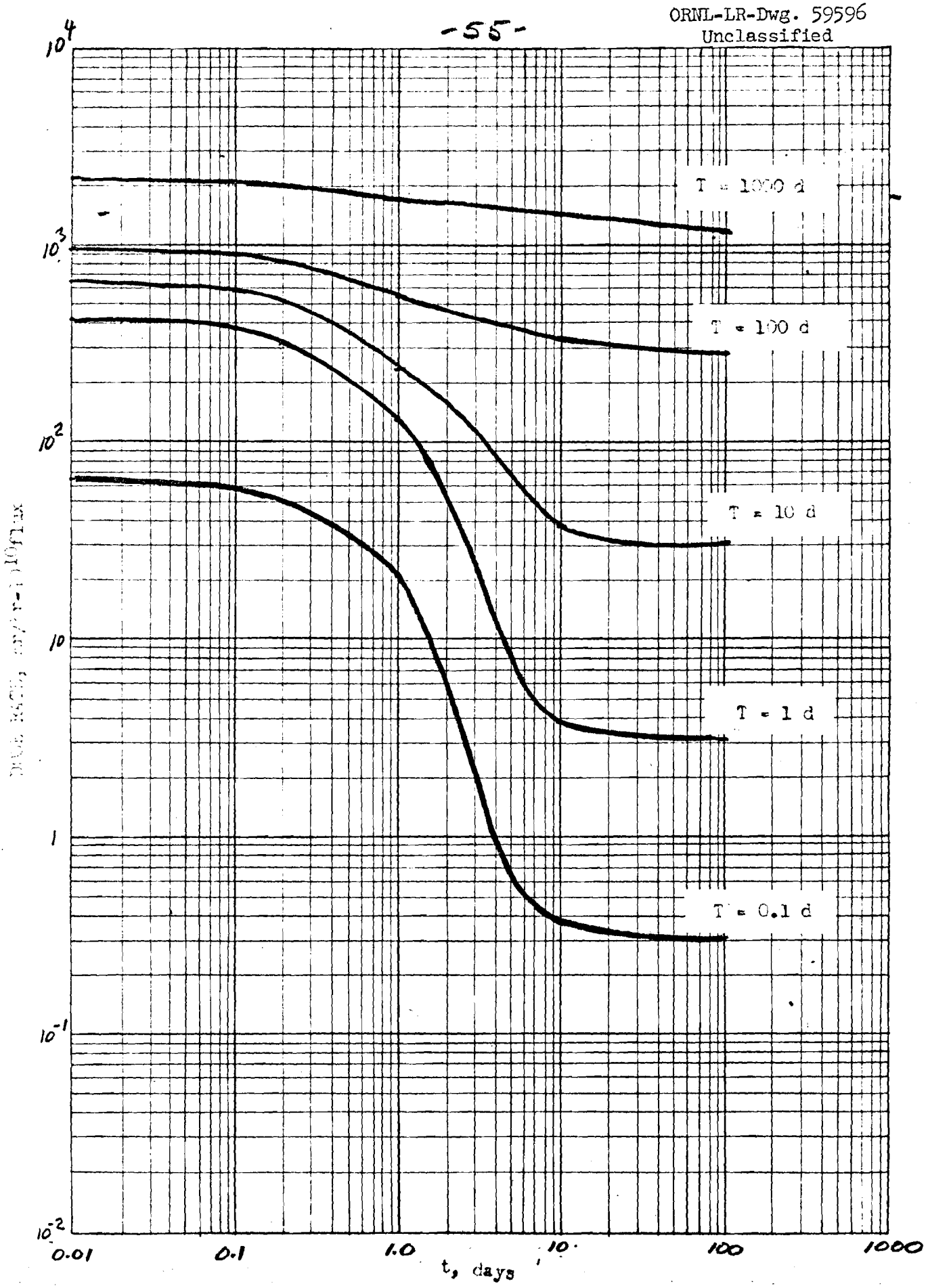

FIGURE 41 ACTIVATION GAMMA DOSE RATE AT THE SURFACE OF A SLAB AS A FUNCTION OF IRRADIATION TIME, T, AND DECAY TIME, t.

MATERIAL: MAGNETITE CONCRETE (FAST FLUX)

ORNL-LR-Dwg. 59597
Unclassified

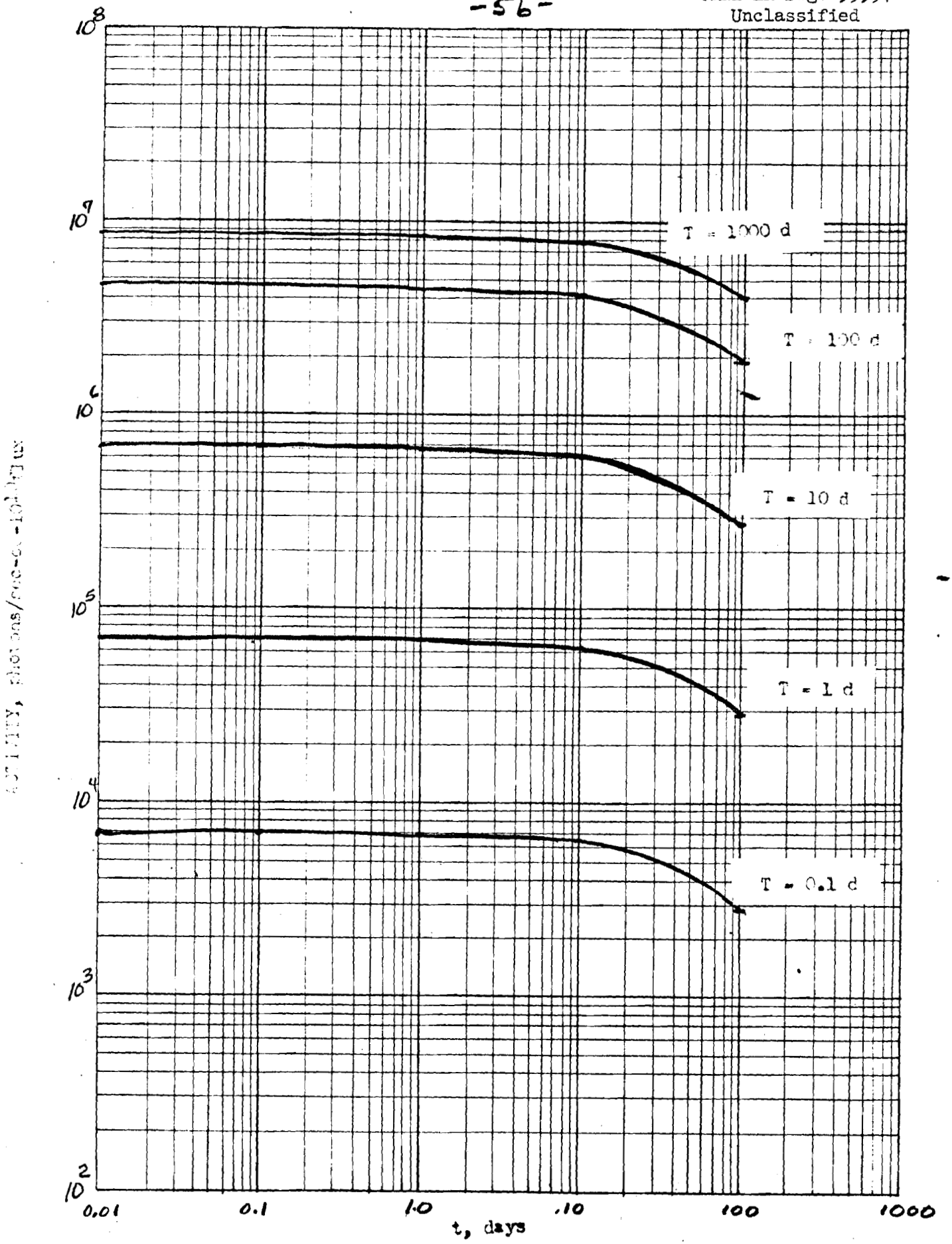

FIGURE 42 ACTIVATION GAMMA ACTIVITY AS A FUNCTION OF IRRADIATION TIME, T, AND DECAY TIME, t.

ORNL-LR-Dwg. 59598
Unclassified

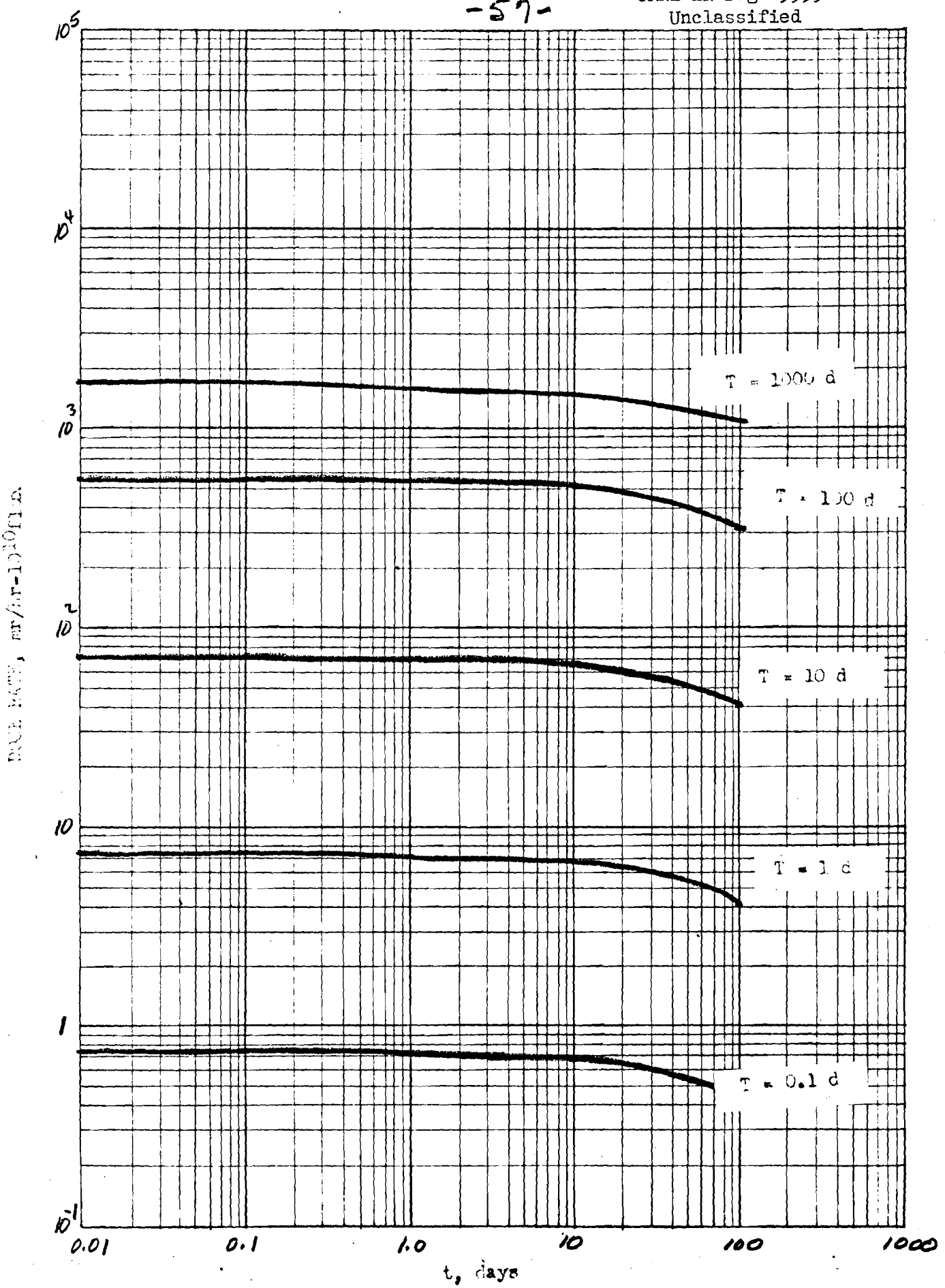

FIGURE 43 ACTIVATION GAMMA DOSE RATE AT THE SURFACE OF A SLAB AS A FUNCTION OF IRRADIATION TIME, T, AND DECAY TIME, t.

MATERIAL: 304L S.St. (FAST FLUX)

ORNL-LR-Dwg. 59599
Unclassified

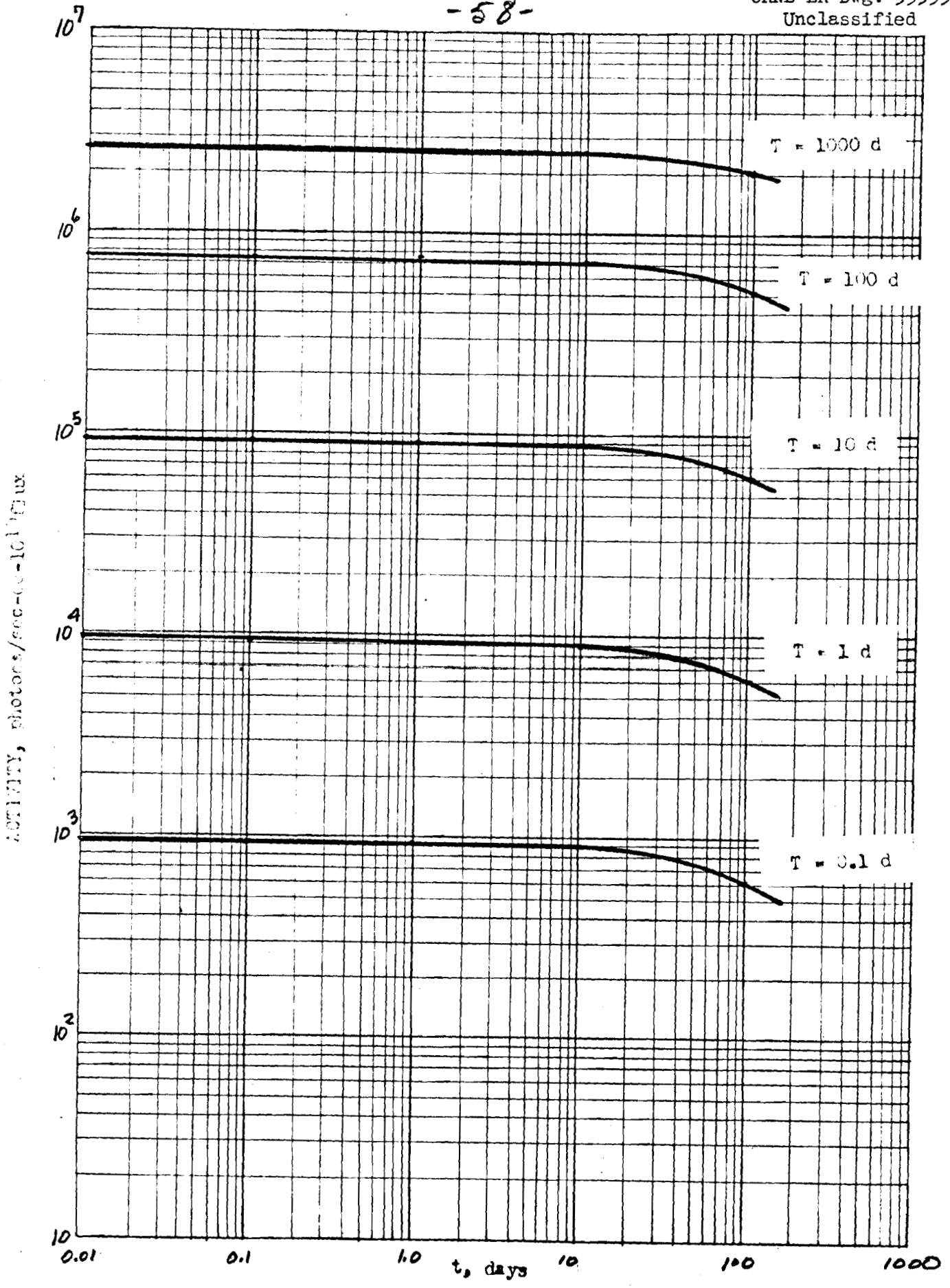

FIGURE 44 ACTIVATION GAMMA ACTIVITY AS A FUNCTION OF IRRADIATION TIME, T, AND DECAY TIME, t.

ORNL-LR-Dwg. 59600
Unclassified

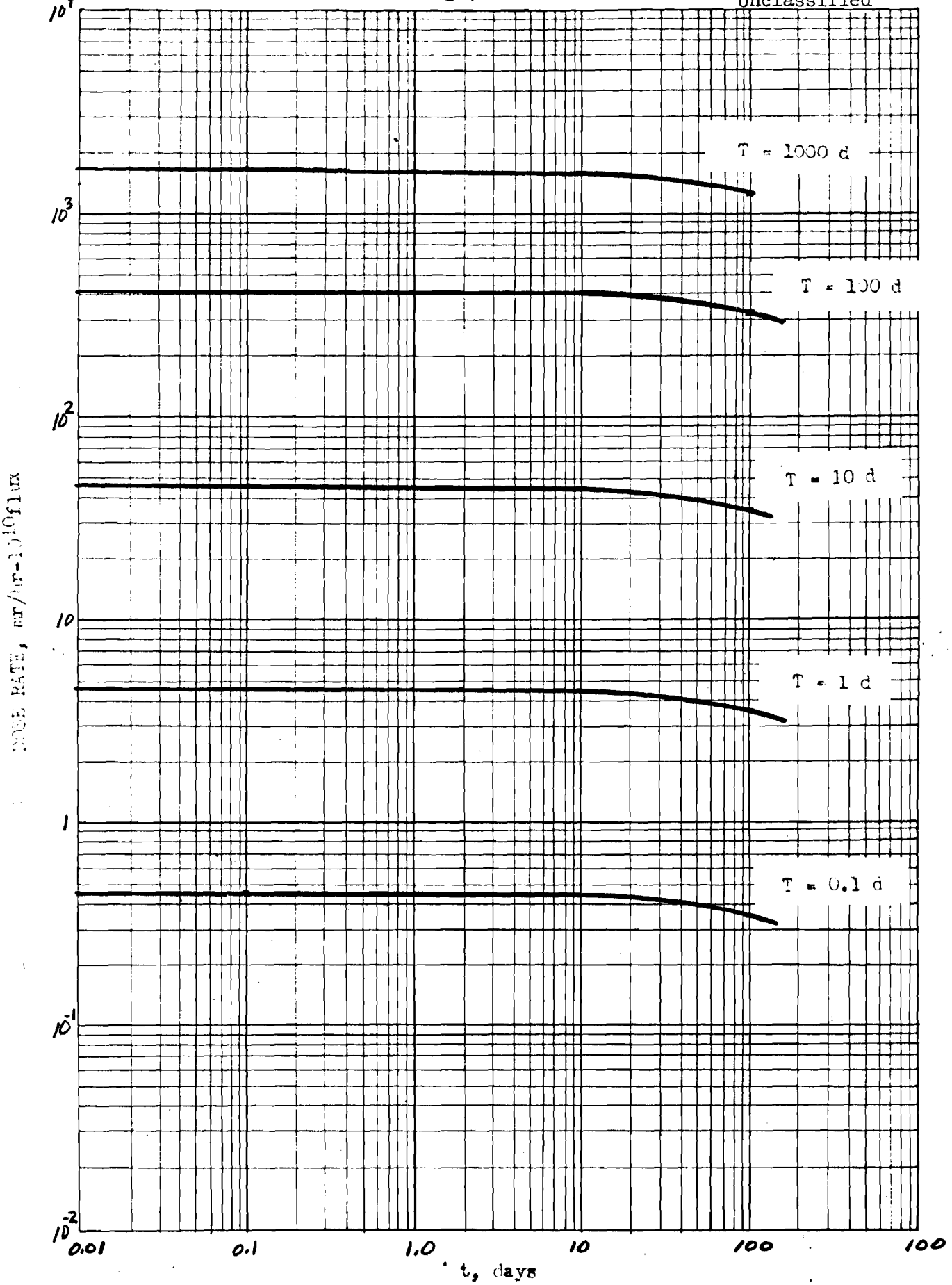

FIGURE 45 ACTIVATION GAMMA DOSE RATE AT THE SURFACE OF A SLAB AS A FUNCTION OF IRRADIATION TIME, T, AND DECAY TIME, t.

MATERIAL: CARBON STEEL (FAST FLUX)

Distribution

1-3. DTIE, AEC
4. M. J. Skinner